EXPERIMENTAL INVESTIGATION OF LOW SALINITY WATER FLOODING TO IMPROVE VISCOUS OIL RECOVERY FROM THE SCHRADER BLUFF RESERVOIR ON ALASKA NORTH SLOPE

By

Yaoze Cheng

A Thesis Submitted in Partial Fulfillment of the Requirements

for the Degree of

Master of Science

in

Petroleum Engineering

University of Alaska Fairbanks

May 2018

APPROVED:

Yin Zhang, Committee Chair
Abhijit Dandekar, Committee Member
Obadare Awoleke, Committee Member
Gang Chen, Committee Member
Abhijit Dandekar, Chair
Department of Petroleum Engineering
Doug Goering, Dean
College of Engineering and Mines
Michael Castellini, *Dean of the Graduate School*

ABSTRACT

Alaska's North Slope (ANS) contains vast resources of viscous oil that have not been developed efficiently using conventional water flooding. Although thermal methods are most commonly applied to recover viscous oil, they are impractical on ANS because of the concern of thawing the permafrost, which could cause disastrous environmental damage. Recently, low salinity water flooding (LSWF) has been considered to enhance oil recovery by reducing residual oil saturation in the Schrader Bluff viscous oil reservoir.

In this study, lab experiments have been conducted to investigate the potential of LSWF to improve heavy oil recovery from the Schrader Bluff sand. Fresh-state core plugs cut from preserved core samples with original oil saturations have been flooded sequentially with high salinity water, low salinity water, and softened low salinity water. The cumulative oil production and pressure drops have been recorded, and the oil recovery factors and residual oil saturation after each flooding have been determined based on material balance. In addition, restored-state core plugs saturated with viscous oil have been employed to conduct unsteady-state displacement experiments to measure the oil-water relative permeabilities using high salinity water and low salinity water, respectively. The emulsification of provided viscous oil and low salinity water has also been investigated. Furthermore, the contact angles between the crude oil and reservoir rock have been measured.

It has been found that the core plugs are very unconsolidated, with porosity and absolute permeability in the range of 33% to 36% and 155 mD to 330 mD, respectively. A produced

crude oil sample having a viscosity of 63 cP at ambient conditions was used in the experiments. The total dissolved solids (TDS) of the high salinity water and the low salinity water are 28,000 mg/L and 2,940 mg/L, respectively. Softening had little effect on the TDS of the low salinity water, but the concentration of Ca^{2+} was reduced significantly. The residual oil saturations were reduced gradually by applying LSWF and softened LSWF successively after high salinity water flooding. On average, LSWF can improve viscous oil recovery by 6.3% OOIP over high salinity water flooding, while the softened LSWF further enhances the oil recovery by 1.3% OOIP. The pressure drops observed in the LSWF and softened LSWF demonstrate more fluctuation than that in the high salinity water flooding, which indicates potential clay migration in LSWF and softened LSWF. Furthermore, it was found that, regardless of the salinities, the calculated water relative permeabilities are much lower than the typical values in conventional systems, implying more complex reactions between the reservoir rock, viscous oil, and injected water. Mixing the provided viscous oil and low salinity water generates stable water-in-oil (W/O) emulsions. The viscosities of the W/O emulsions made from water-oil ratios of 20:80 and 50:50 are higher than that of the provided viscous oil. Moreover, the contact angle between the crude oil and reservoir rock in the presence of low salinity water is larger than that in the presence of high salinity water, which may result from the wettability change of the reservoir rock by contact with the low salinity water.

TABLE OF CONTENTS

LIST OF FIGURES

Figure **Page**

LIST OF TABLES

Table **Page**

ACKNOWLEDGEMENTS

I would like to take this opportunity to thank my advisor, Dr. Yin Zhang, for being a constant source of advice and support, without which the completion of this thesis would not have been possible. I also thank Dr. Gang Chen, Dr. Obadare Awoleke, and Dr. Abhijit Dandekar for being my thesis committee members and for their help and guidance.

I am grateful to Hilcorp for providing crude oil samples, preserved cores, and water samples. I appreciate the equipment and necessary help provided by Corelab. The financial support provided to me by Hilcorp is greatly appreciated. Finally, I would like to thank all my friends and professors here who made my stay in Fairbanks a very enjoyable experience.

1. Introduction

Alaska North Slope (ANS) is one of the largest world-class hydrocarbon resource basins with the largest producing oil field in North America, Prudhoe Bay Oil Field, whose amount of recoverable oil is more than twice the next largest oil field in the United States, East Texas Oil Field (Young et al. 2010; Benavides 2015). However, most of the hydrocarbon reserves on ANS are viscous and heavy oil, whose API gravity ranges from 15 to 22 degrees and 8 to 12 degrees, respectively (Attanasi and Freeman 2014). The total estimated sizes of viscous and heavy oil resources on ANS are somewhere around 12 billion barrels of Original-Oil-In-Place (OOIP) and 18 billion barrels of OOIP, respectively (Young et al. 2010; Pospisil 2011).

Although vast viscous and heavy oil reserves discovered on ANS is encouraging, the task of producing these resources commercially in an Arctic environment has challenged oil companies for about half of the century (Attanasi and Freeman 2014). Without a doubt, viscous and heavy oil are highly valuable assets, and it is the interest of the petroleum industry to work for decades on developing new methods that can lead to producing these vast oil reserves commercially (Attanasi and Freeman 2014).

Currently, many techniques have been proposed to increase recovery factor to lead sustained profitable production of viscous and heavy oil:

(1) Waterflood.

Waterflood is the first enhanced oil recovery process that was used on ANS to produce viscous and heavy oil. It is still reported as the current EOR process in Schrader Bluff

formation development (Attanasi and Freeman 2014) since the oil pool is relatively at early production stage. However, water flooding is insufficient due to fingering resulting in low oil recovery (no more than 20%), with some oil pools having a recovery rate of less than 10% (Targac 2005; Paskvan et al. 2016).

(2) Chemical EOR.

Polymer flood and Alkaline-Surfactant-Polymer (ASP) flood are under consideration to extract viscous oil on ANS via type pattern model (TPM) evaluation (Paskvan et al. 2016). Polymer flood is attractive when producing less viscous oil (less than 50 cP), which may result in 6% to 10% recovery improvement (Paskvan et al. 2016). ASP flood is also found to be a potentially feasible method to extract less viscous oil on ANS, which may result in 20% recovery enhancement (Paskvan et al. 2016). Nonetheless, both EOR processes are limited due to the high material costs and processing and design problems.

(3) Steam injection.

The steam-based recovery process has been practical and commercially developed in other places all over the world, especially for higher viscous oil extraction in shallower zones (Paskvan et al. 2016). Although steam-based techniques have been considered as the most efficient method to recover viscous and heavy oil, steam injection is not viable on ANS (Targac et al. 2005; Attanasi and Freeman 2014). That is attributed to the fact that the increase of subsurface temperature may result in thawing the permafrost. In addition, the increase of fluid pressure results in improved solubility of potentially hazardous components contained in the underground formations, as well as high well

costs, heat loss, instability, and other dangerous conditions for well and surface facilities located on the permafrost (Targac et al. 2005; Attanasi and Freeman 2014).

(4) Water-alternating-gas (WAG).

The WAG EOR process is more attractive to produce viscous and heavy oil on ANS since near-well-bore viscosity can be reduced significantly at producers, resulting in additional oil recovery (McKean et al. 1999). A newer WAG method called Viscosity Reducing WAG (VR-WAG) was first introduced in 2004 to be applied on ANS (McGuire et al. 2005; Attanasi and Freeman 2014). As viscosity-reducing injectant (VRI), such as CO_2 or hydrocarbon gas, is injected into a viscous and heavy oil reservoir, oil viscosity can be reduced up to 90%, leading to additional oil recovery of up to 20% (McGuire et al. 2005; Targac et al. 2005; Paskvan et al. 2016). In the beginning, produced natural gas was selected to be the VR agent in the VR-WAG process, which can swell the viscous and heavy oil in the reservoir and reduce its viscosity, resulting in ultimate recovery improvement (Targac et al. 2005). More recent research shifts natural gas liquid (NGL) injection to CO_2 injection and CO_2 enriched with NGL injection in the VR-WAG process since miscibility is more possible to be achieved and oil viscosity can be reduced significantly (Ning et al. 2011; McGuire et al. 2005; McKean et al. 1999). However, same as with water flood, fingering will happen during VR-WAG injection where viscosity of oil is much higher, so the VR-WAG is not viable in the process of extracting a much higher viscous oil (McGuire et al. 2005). Besides, the early gas breakthrough and reduction of macroscopic sweep generally result in lower additional recovery than the prediction (Christensen et al. 2001; Awan et al. 2008).

(5) Cold Heavy Oil Production with Sand (CHOPS).

The CHOPS is a novel extraction strategy that introduced to ANS by BP (Yong et al. 2010). This new EOR method is employed for viscous and heavy oil production from poorly consolidated or unconsolidated sand reservoirs where sand production is allowed (Yong et al. 2010; Nassir et al. 2015). A CHOPS pilot test was conducted on ANS in 2010, with the result of the pilot production test showing that viscous and heavy oil can be technically developed using this extraction technology (Yong et al. 2010; Chmielowski 2013). Although CHOPS is a promising technology to extract vast viscous and heavy oil reserves on ANS, it is still restricted due to high sand production.

Although many EOR techniques have been proposed to recover the ANS viscous and heavy oil resources, these methods have shown limited recovery factors. Therefore, a more feasible and efficient extraction method is needed to produce viscous and heavy oil on ANS. Recently, Low Salinity Water Flood (LSWF) has been recognized as a promising technique to enhance oil recovery (Nasralla et al. 2014; Chandrashegaran 2015; Zeinijahromi et al. 2015). The LSWF is a relatively recently developed EOR process of injecting low salinity brine into sandstone and/or carbonate reservoirs to improve microscopic displacement efficiency (Muggeridge et al. 2013). The EOR performance of injecting low salinity water in the field application showed significant benefits, with a reduction in residual oil saturation of somewhere between 5.6% and 7.6% (Buikema et al. 2012). Many studies have been conducted to investigate the governing physical and chemical mechanisms for this increase in recovery, but they are not yet agreed upon. Generally, it is believed that some form of interaction between the rock, oil, and brine leading to changes in wettability and oil/water interfacial tension is involved (Lager et al. 2008). Since

there is still no consistent conclusion on the mechanisms of LSWF, there is no common reservoir screening criteria for LSWF. But, in general, certain clay content is essential for efficient LSWF (Fjelde et al. 2014; Shehata et al. 2017). Clay surface remaining divalent cations help adsorb polar oil components that can be released during LSWF (Fjelde et al. 2014; Shehata et al. 2017). Therefore, prior to any field application, detailed laboratory experiments must be conducted to evaluate the LSWF efficiency in the to-be-implemented reservoirs. Most recently, the LSWF is attracting much more attention as a way to recover viscous and heavy oil.

2. Literature Survey

2.1 Introduction of low salinity water flooding (LSWF)

Injection of low salinity water (LSW) has been widely practiced because the LSW sources are available and relatively cheaper compared to the other materials. LSWF is a form of EOR process different from conventional water flooding in that is uses water containing a low concentration of dissolved salts as a flooding medium to enhance oil recovery, which is also known as low salinity effect. (McGuire et al. 2005; Sheng 2014). Generally, water with total dissolved solids (TDS) in a range of 1,000-2,000 ppm is considered as LSW (Austad et al. 2010). However, the low salinity effect (LSE) has been observed when TDS in the injected water is as high as 5,000 ppm (Austad et al. 2010). In comparison, seawater salinity is about 35,000 ppm and formation water salinity can exceed 200,000 ppm (Dept. of the Interior 1973).

LSE was first observed through adjusting pH and sodium content of injected water in 1959 and was applied in the oilfield tests in 1962 (Wagner and Leach 1959; Leach and Wagner 1962). After the first laboratory investigations of the impact of water composition on oil recovery in 1959 and 1967, no further consistent laboratory studies of the effect were conducted until the 1990s since oil companies were focusing on producing light oil (Jadhunandan and Morrow 1995; Tang and Morrow 1999). Scientific investigation of spontaneous imbibition of water in the formation rock led to a more refined study measuring the effects of injected brine composition on oil recovery (Yildiz and Morrow 1996). Filoco and Sharma (1998) proposed that the residual oil saturation was dependent on the salinity of the brine used, and that much higher oil recoveries can be obtained by injecting lower salinity brines. Morrow and Tang continued this work to

further gauge the influence of brine composition and fine migration as well as brine cation valency and salinity on oil recovery (Tang and Morrow 1999). BP researchers noted that laboratory tests had shown incremental oil production of 2% to 10% with LSW containing 2,600 ppm dissolved content flooding through cores without causing formation damage (Lager et al. 2008). The experimental data from Zahid et al. (2012) stated that LSE was also effective at ambient temperature, while an increase in oil recovery by LSWF was observed at high temperature (90^0C). Kulathu et al. (2013) concluded that low salinity cyclic water flooding resulted in better oil recovery and earlier residual oil saturation under a shorter injection period compared to continuous water injection, while a decrease in brine salinity can yield higher oil recovery and lower residual oil saturation. Since then, many tests have been conducted to investigate the LSE on water flooding in the oil recovery process (Sheng 2014). Most of the results showed that higher oil recovery could be achieved when the salinity of injected water is much lower than that of the formation water (or produced water) (Sheng 2014). Also, work done by Morrow and his co-workers showed that a concentration of 1,500 ppm NaCl could result in a sharp increase in oil recovery and pressure drop, while their simulation run showed that 2,000 ppm of salinity was optimal for most rock types and at least an additional 4% of oil could be produced (Chandrashegaran 2015).

Empirical studies supported by BP had proven that the mechanisms of LSWF were particularly relevant to the removal of divalent cations, such as Mg^{2+} and Ca^{2+}, from the injected water (Haagh et al. 2017). Studies found that these cations have a strong tendency to adsorb to the silica and clay surfaces that are plentiful in sandstone (or limestone) reservoirs (Haagh et al. 2017). The surface charge can be reversed, which can make the rock surface more oil-wet by

adsorption of divalent cations. Further, more oil will be trapped in the reservoir since polar oil components are bound to the rock surfaces (Haagh et al. 2017). Removing the divalent cations from the injection water (also decreasing the overall salinity in the meantime) can release the surface-bound polar oil components (Haagh et al. 2017). Clearly, oil recovery factor can be enhanced using LSWF.

After LSWF, some changes to the rock and effluent water have been observed. The injection of LSW results in a pH increase of 1-3 pH units in the effluent water, but it has not been verified that an increase in pH is necessary to the observed LSE (Austad et al. 2010). In some cases, LSWF may also produce additional fines, but fines production is not essential for LSE (Lager et al. 2008). Also, related to fines production, an increase in injection pressure is usually detected when switching to injection of LSW, which might be a result of a decrease in permeability due to fines migration or formation of emulsion (Webb et al. 2007). Correspondingly, during LSW injection, permeability reduction for water results in diverting the water to an unswept zone and delaying water breakthrough (Zeinijahromi et al. 2015).

Most recently, the LSWF has been considered as a promising and accepted technology for improving oil recovery. Although the general consensus is that LSWF increases oil recovery due to a change in the formation rock wettability, the exact mechanism that leads to increased oil production is still a matter of debate (McGuire et al. 2005; Nasralla et al. 2011; Chandrashegaran 2015; Zeinijahromi et al. 2015). Jerauld et al. (2006) proposed that the increased oil recovery rate was directly proportional to kaolinite content on the rock surface. Ashraf et al. (2010) and Yousef et al. (2011) suggested that wettability alterations due to multi-ion exchange, double

layer expansion, pH increase, reduction of interfacial tension, and fine migration are the main contributors to oil recovery improvement in LSWF. Other studies have reported that compositions of brine and crude oil are also contributing to the increase of oil recovery (Filloco and Sharma 1998; Alotaibi and Nasr-El-Din 2009; Pu et al. 2010; Fjelde et al. 2014; Alshakhs and Kovscek 2015; Alshaikh and Mahadevan 2016).

Researchers are continuing to try to pinpoint the various explanations, but successful LSWF has been proven to be an effective method of improving oil recovery in the laboratory and on the fields. Most importantly, LSWF has been proven to be a technology that can work on ANS (McGuire et al. 2005).

2.2 Theories of LSWF

2.2.1 Wettability alteration

It has been generally recognized that wettability alteration is the essential cause of LSE. And LSW injection can significantly increase oil recovery factor at the low water-wet condition (mix-wet system) (Yousef 2010).

The contact angle is one of the methods that evaluate the wetting characteristics (wettability) of solid surfaces (Alotaibi 2010). This method is usually conducted by using a small piece of rock sample whose surface should be smoothed and polished to avoid any hysteresis issue and two immiscible fluids (Alotaibi 2010). The wettability is classified as water-wet (0^o-75^o), mix-wet (75^o-115^o), and oil-wet (115^o-180^o), respectively (Anderson 1986). According to Alotaibi's (2010) work, results of contact angle and atomic force microscope (AFM) measurements

demonstrated that the presence of brine was critical to alter water-wet to oil-wet, which can increase contact angle of the existence of brine film from 41° to 144°.

Alotaibi et al. (2010) found that the contact angle reduced slightly with the decrease in salinity (water samples changed from formation brine to seawater), and the wettability changed dramatically towards strong water-wet when aquifer water with TDS of 5,436 ppm was applied. Also, rock mineralogy was found to be another critical factor in determining the effect of low salinity brine on the contact angle (Alotaibi 2010). Other laboratory core flooding tests by Yousef (2010) showed that oil recovery was increased due to LSW injection resulting in wettability alteration from mixed-wet to water-wet, which is significant and persistent.

The wettability alteration by LSWF in carbonate formations has been investigated recently (Gupta et al. 2011). Review of experimental results in the published work indicates wettability change due to the interaction of Na^+, Cl^-, Ca^{2+}, Mg^{2+}, SO_4^{2-} and crude oil carboxylate ions ($R\text{-}COO^-$) with the rock, resulting in oil recovery improvement (Gupta et al. 2011; Al-Harrasi et al. 2012; Austad et al. 2012; Yousef et al. 2012; Yi and Sarma 2012). A study by Zekri et al. (2012) found that contact angle alters with an injection time of LSW, while it concluded that wettability change is the main factor to enhance oil recovery in carbonate reservoirs by injecting low salinity brine. Romanuka et al. (2012) published their work showing that the oil recovery can be increased in carbonate reservoirs, altering wettability to a more water-wet state. In addition, Fjelde et al. (2013) proposed that LSWF changed the wettability from oil-wet to less water-wet, while the production time was much longer than that of formation water flooding. Based on the previous study, Alameri et al. (2014) conducted four seawater flooding tests in heterogeneous

low permeability carbonate core plugs, which were followed by LSW injection, and found that LSWF yielded a significant additional recovery (about 8% OOIP) after seawater flooding due to wettability alteration (Alameri et al. 2014). Another study conducted by Al-Shalabi et al. (2015) on the potential of LSWF in carbonate reservoirs confirmed that oil recovery could be improved by changing rock wettability to more water-wet. Most recently, Alshaikh and Mahadevan (2016) further demonstrated that the increased water-wet conditions resulted from a moderate reduction in salinity.

2.2.2 Fine migration

Some researchers propose that the enhanced oil recovery rate by injecting LSW is related to the presence of clay particles in porous media (Tang and Morrow 1999; Zahid et al. 2012; Bedrikovetsky et al. 2013).

The attempt to explain the mechanism of LSWF by fine mobilization was first presented by Tang and Morrow (1999) after they found fines were moved during LSWF on Berea core samples. During the injection of LSW, the fine migration resulting in exposure of underlying surfaces was observed, which made the core sample more water-wet, so an additional oil recovery was produced. They also reported a reduction in permeability when LSW replaced initial high salinity brine (Tang and Morrow 1999). Zahid et al. (2012) agreed that the fine migration or dissolution effects may have occurred and may contribute to the increase in oil recovery because of the increase in pressure drop. Later, Bedrikovetsky et al. (2013) emphasized that oil recovery was enhanced due to induced fine migration during displacement of oil by LSW injection. Fines are remobilized by injecting LSW, which may reduce water flux in higher permeable layers and

increase the oil flux due to formation damage and consequent reduction in water relative permeability, increasing oil recovery (Bedrikovetsky et al. 2013).

2.2.3 pH change

Based on published papers and experimental results, pH change is proposed to be a potential mechanism for oil recovery improvement by LSWF (Austad et al. 2010; Fjelde et al. 2013). At reservoir conditions, the pH of formation water is around 5 due to dissolved acidic gases like CO_2 and H_2S, resulting in adsorption of acidic and protonated basic components from crude oil, and cations from formation water like Ca^{2+} onto clay minerals (Austad et al. 2010). Injection of LSW, which results in desorption of Ca^{2+}, will increase the pH of water, leading to desorption of organic components from the clay due to the fast reaction between OH^- and the adsorbed acidic and protonated basic components (Austad et al. 2010). Then the wetness is changed to be more water-wet, and oil recovery is improved.

2.2.4 Impact of interfacial tension (IFT)

It has been found that IFT can be reduced by injecting an optimum salinity of water, resulting in enhanced oil recovery (Alotaibi and Nasr-El-Din 2009). In Alotaibi and Nasr-El-Din's summary (2009), the IFT decreased initially due to the decrease in brine salinity, while the IFT increased with further dilution of brine with distilled water. Xu (2005) presented that dilution of formation water (50% formation brine in DI water) increased IFT. Further, the IFT measurement conducted by Alameri et al. (2014) showed that the oil-brine IFT increased with the reduction in salinity. It can be concluded that lowering the brine concentration will increase the IFT after a critical point. In order to maximize oil recovery, optimum brine salinity should be applied.

2.2.5 Expansion of electrical double layer

Ligthelm et al. (2009) suggested that reduction in salinity will increase the size of the ionic double layer between the clay and oil interfaces, which release organic materials, resulting in additional oil recovery.

2.2.6 Multi-ion exchange

Another explanation for improved oil recovery by injecting LSW is the multi-component ionic exchange (MIE) (Fjelde et al. 2013). As mentioned, one of the causes for the rock surface to be oil-wet is ionic binding between the oil and mineral surface, through multi-valent cations such as Ca^{2+}, Mg^{2+}, and Fe^{2+} (Fjelde et al. 2013). A reduction of the concentration of these divalent cations due to injection of lowered salinity water results in the ion-bound oil being released from the mineral surface. Therefore, MIE would take place by injecting LSW, removing organic polar compounds and organo-metallic complexes that can cause reservoir rocks to be more oil-wet in order to generate a more water-wet surface. Thus, oil recovery can be improved (Fjelde et al. 2013).

2.3 Application criteria

It has been widely recognized that LSWF can lead to higher oil production in the field. However, LSWF may not be applied to all oil reservoirs as an enhanced oil recovery technique. For LSWF to be effective, some necessary conditions must exist. The requirements for successful LSWF mainly include the following: the porous reservoir rock contains clay, the oil composition contains polar components, the presence of connate water contains divalent cations such as Ca^{2+}

and Mg^{2+}, and initial formation water must be present in the rock (Tang and Morrow 1999; Austad et al. 2010; Morrow and Buckley 2011).

The first condition is that the reservoir needs to be composed of a porous medium containing some clay. Pure carbonates are not good candidates for LSWF, but there is some evidence that sandstones containing dolomite crystals can still benefit from LSWF (Pu et al. 2008). Sandstone reservoirs are porous, and they are good candidates for LSWF if they also contain some clay (Pu et al. 2008). Seccombe et al. (2010) published a simple linear correlation between additional oil recovery due to LSW injection and the proportion of clay content in the rock for Endicott Field on Alaska North Slope, which indicates that higher clay content proportion will cause higher additional oil recovery rate. Pu et al. (2010) reported that 9.5% additional original oil in place was produced by injecting coalbed methane water with low salinity into sandstone cores containing very low clay content. Another performance of LSWF examined by Rezaei Doust et al. (2010) at North Sea Offshore Field showed that additional oil recovery rate decreased from 6% to 2% due to the reduction of clay content (from 16 wt% to 8 wt%) of the cores. Fjelde et al. (2014) found that the clay content plays a vital role in the LSE: it is not only the concentration of the clay but also the distribution of the clay that influences the LSE. Shehata et al. (2017) investigated the effects of clay content and rock permeability. Instead of clay fraction, the amount and surface area of each type of clay are the important roles that affect the additional oil recovery factor, while the presence of kaolinite was believed to be vital for the success of LSWF (Shehata et al. 2017).

The second condition is that the oil must contain polar components. Laboratory results showed that when crude oil has high concentration of polar components, injecting LSW could decrease the concentration of divalent cations on the clay, leading to low retention and hence changing the wettability to be more water-wet, (Fjelde et al. 2014). Later, Yang et al. (2015) suggested that desorption of polar crude oil components from mineral surface on the rock could lead to the wettability altering to be more water-wet during LSWF, which contributes to an increase of oil recovery. Recently, composition analysis of the oil produced during the LSWF conducted by Sohrabi et al. (2017) indicated desorption of natural surface-active compounds of the crude oil from the rock surface during LSWF, resulting in improved oil recovery.

The third condition is that initial connate water must exist within the formation for LSWF to result in improved oil production. Not only must there be formation water, but it must contain divalent cations like Ca^{2+} and Mg^{2+} (Lager et al. 2006). Morrow and Buckley (2011) found that oil recovery would be maximized by injecting either LSW or high salinity water if connate water is LSW, while a 6% higher recovery factor is found with LSW injection than with either high salinity water or moderate salinity water injection when the connate water is high salinity water. The visualization study, using reservoir-condition micro models, implied that LSE contributes to additional oil recovery when a mixed-wet system and high salinity connate water exist (Emadi and Sohrabi 2013). Lately, Shehata and Nasr-El-Din (2015; 2017) evaluated the effect of divalent cations (Ca^{2+} and Mg^{2+}) and monovalent cations (Na^{+}) in connate water. Core flooding tests showed that core plugs saturated with connate water containing divalent cations of Ca^{2+} and Mg^{2+} yielded more oil than the core plugs saturated with monovalent cations of Na^{+} (Shehata and Nasr-El-Din 2015; Shehata and Nasr-El-Din 2017).

2.4 Objectives of the study

- To determine the residual oil saturation after flooding with the high salinity water, LSW, and softened LSW, successively;
- To measure the water-oil relative permeabilities for the Schrader Bluff sand using the high salinity water, LSW, and softened LSW, respectively.

3. Background Review

3.1 Geological background

Alaska North Slope's (ANS) deposited viscous oil with viscosity in a range of 20 to 650 cp and heavy oil with viscosity values of greater than 10,000 cp in the Schrader Bluff and Ugnu formations are shown in *Figure 3.1*. The Schrader Bluff sand holds mostly viscous oil while Ugnu sand retains heavy oil (Seccombe et al. 2005). Since the target of development is producing viscous oil from Schrader Bluff formation (McGuire et al. 2005), only Schrader Bluff formation will be described briefly.

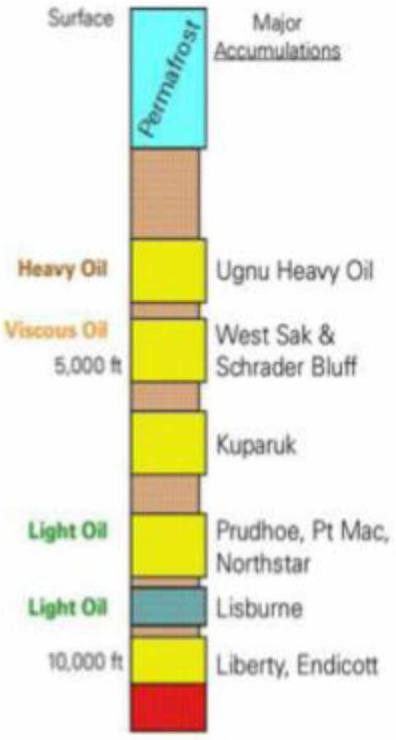

Figure 3.1 ANS Stratigraphic Column (Paskvan et al. 2016)

Stratigraphy. The Schrader Bluff sand is located at "Shallow Sands," which are adjacent to the permafrost (Hallam et al. 1992). The Schrader Bluff formation was deposited in a shallow marine sand complex formed during the Late Cretaceous-aged geologic time, which is very friable and poorly consolidated (Bidinger and Dillon 1995; McKean et al. 1999; Li et al. 2003; Seccombe et al. 2005). The Schrader Bluff sand is classified into two stratigraphic intervals, the O-sands and the N-sands, from the deepest to shallowest. Some researchers subdivide the reservoir into three major sands, the OB, OA, and N (Bidinger and Dillon 1995; McKean et al. 1999; Seccombe et al. 2005; Paskvan et al. 2016).

Sedimentology. The Schrader Bluff sand is made of 8 productive horizons with a total thickness of approximately 200 feet, formed predominantly of quartz and other minerals (Bidinger and Dillon 1995; Seccombe et al. 2005; Paskvan et al. 2016).

Structure. The depth of Schrader Bluff formation varies from 3,500 feet to 5,000 feet, with an average depth of 4,000 feet total vertical depth subsea (TVDss), which is overlaid by Ugnu formation as shown in *Figure 3.1* (Seccombe et al. 2005; Attanasi and Freeman 2014; Paskvan et al. 2016).

3.2 Reservoir description

Oil characteristics. The viscosity of crude oil ranges from 20 cP to 650 cP, with gas/oil ratio varying from 80 to 350 SCF/STB (McKean et al. 1999; Guler et al. 2001; Seccombe et al. 2005; Attanasi and Freeman 2014). The oil gravity varies from 14° to 21.5°, with an average of 18° (Bidinger and Dillon 1995; Khataniar et al. 1999; McKean et al. 1999). The oil saturation is

between 55% and 73%, with little aquifer support due to variation in the oil-water-contact (OWC) (McKean et al. 1999; Guler et al. 2001; Attanasi and Freeman 2014).

Porosity and permeability. The porosity ranges from 25% to 32%, with an average value of 28% (Seccombe et al. 2005; Attanasi and Freeman 2014). The permeability lies between 10 mD and 300 mD in the O-Sands and increases to the range of 200 mD to 3000 mD in the N-Sands, with an average permeability of 171 mD (Seccombe et al. 2005; Attanasi and Freeman 2014).

Reservoir temperature and pressure. The reservoir temperature lies in the range of 80°F to 86°F (Bidinger and Dillon 1995; McKean et al. 1999; Guler et al. 2001; Seccombe et al. 2005). The reservoir pressure is between 1,400 psi and 1800 psi, with a commonly accepted value of 1750 psi (Bidinger and Dillon 1995; McKean et al. 1999; Guler et al. 2001; Seccombe et al. 2005).

3.3 Production history

Most of the Schrader Bluff sand was found in August 1969 in Milne Point Unit (MPU) but not commercially developed until March 1991 (Bidinger and Dillon 1995). The average initial production rate peaked at 3,700 barrels of oil per day (BOPD) in October 1991 and averaged at around 350 BOPD, with an average initial gas-oil-ratio (GOR) of 180 SCF/STB (Bidinger and Dillon 1995). The production rate was first reduced to 2,850 BOPD by the middle of 1993 and then declined to a 200 BOPD average with a GOR of 450 SCF/STB in 1994 (Bidinger and Dillon 1995). In early 1994, the production expanded significantly, with peak production at 23.9 MBOPD in 2003 (Attanasi and Freeman 2014). In 1999, a portion of Schrader Bluff sand sited at

Prudhoe Buy Unit (PBU) was under development, with cumulative production around 33 million barrels and daily production at 14 MBOPD (Attanasi and Freeman 2014). A part of Schrader Bluff sand located in Nikaitchuq Unit (NU) was found in 2004 and started commercial production in 2011, with production rates averaging 5.5 MBOPD (Attanasi and Freeman 2014). By 2016, through extraction methods including water flooding, WAG, and CHOPS, approximately 150 million barrels of viscous oil had been extracted from ANS, indicating that recovery factor of viscous oil is only about 1% (Attanasi and Freeman 2014; Paskvan et al. 2016).

4. Experimental Method

4.1 Experimental Material

4.1.1 Oil Samples

The provided oil samples were from the Milne Point Unit and had a viscosity of 63 centipoise (cp) and density of 0.9633 g/cm3 (15.39° API).

4.1.2 Water Samples

The high salinity water and LSW were provided for flooding. The high salinity water had a salinity of 28,000 mg/L, while the salinity of the LSW was 2,940 mg/L. The high salinity water contained much higher concentrations of Ca^{2+} and Mg^{2+} when compared to the LSW. However, the LSW had much higher concentrations of Na^{+} when compared to the high salinity water. The pH of the LSW was 8.02, which is slightly higher than that of the high salinity water.

4.1.3 Preserved Core Samples

Two one-foot-long preserved cores with diameter of 3.37 inches were provided for the core flooding experiments and relative permeability measurements. One preserved core was from the interval between 3,901 feet to 3,902 feet, while the other one came from the interval between 3,923 feet to 3,924 feet. *Figure 4.1* shows the picture.

Figure 4.1 Preserved Cores

4.1.4 Sodium Carbonate (Na_2CO_3)

Sodium carbonate, also known as soda ash, was used to soften the LSW by precipitating Ca^{2+} and Mg^{2+} out. The CO_3^{2-} from Na_2CO_3 can react with Ca^{2+} and Mg^{2+} to form $CaCO_3$ and $MgCO_3$, which are insoluble or very slightly soluble in water.

4.1.5 Toluene and Alcohol

Typically, in order to clean cores more effectively, varying mixtures of solvents are used. In this case, a mixture of toluene and alcohol was applied to clean the core sample. The mixture was made by adding alcohol into prepared toluene to create an alcohol-toluene ratio of 1:1.

4.2 Experimental Equipment

4.2.1 Coring System

The cooling method used for the coring system's cutting blade and coring bit (see *Figure 4.2*), which are used to cut and drill out the core plugs from the preserved cores, is compressed air directed at the cutting surfaces. The reason for selecting this cooling method is to ensure the ability to obtain core plugs that represent the original state and to keep them saturated with oil while minimizing physical alteration (such as water saturation change if a water cooled system has been selected) of the core plugs during coring of the preserved cores.

Figure 4.2 Coring System

4.2.2 AFS-300 Reservoir Conditions Auto-Flood Core Flooding System

An AFS-300 reservoir conditions auto-flood core flooding system, shown in *Figure 4.3*, is utilized to conduct the core flooding experiments and measure relative permeability curves. The high temperature core flooding experiment apparatus designed by Corelabs is assembled and modified for the experimental runs. The equipment is designed to operate at temperatures up to 400°F (204°C).

Figure 4.3 AFS-300 Reservoir Conditions Auto-Flood Core Flooding System

4.2.3 Core Cleaning System (Dean–Stark Extraction Method)

Dean–Stark extraction, shown in *Figure 4.4*, is employed to clean core plugs that are flooded during the core flooding experiments. The fluid saturations and core plug porosity could be

determined by use of this distillation extraction. The water in the core plugs will be vaporized by boiling solvent (at temperatures as high as 110°C), then condensing and collecting the vapor in a calibrated tube. The water volume of the condensed vapor is measured in this way. The solvent is also condensed, then flows back through the core plugs to remove the oil. This closed process is repeated during the extraction. Extraction is continued for about 72 hours to make sure that the core plugs are completely cleaned. The weight of the core plugs is measured before and after the extraction process. Then, the volume of oil is calculated from the loss in weight of the sample minus the weight of the water removed from it using the measured density of the oil. Saturation is calculated from the fluid volumes, while porosity is calculated from the weight and volumes.

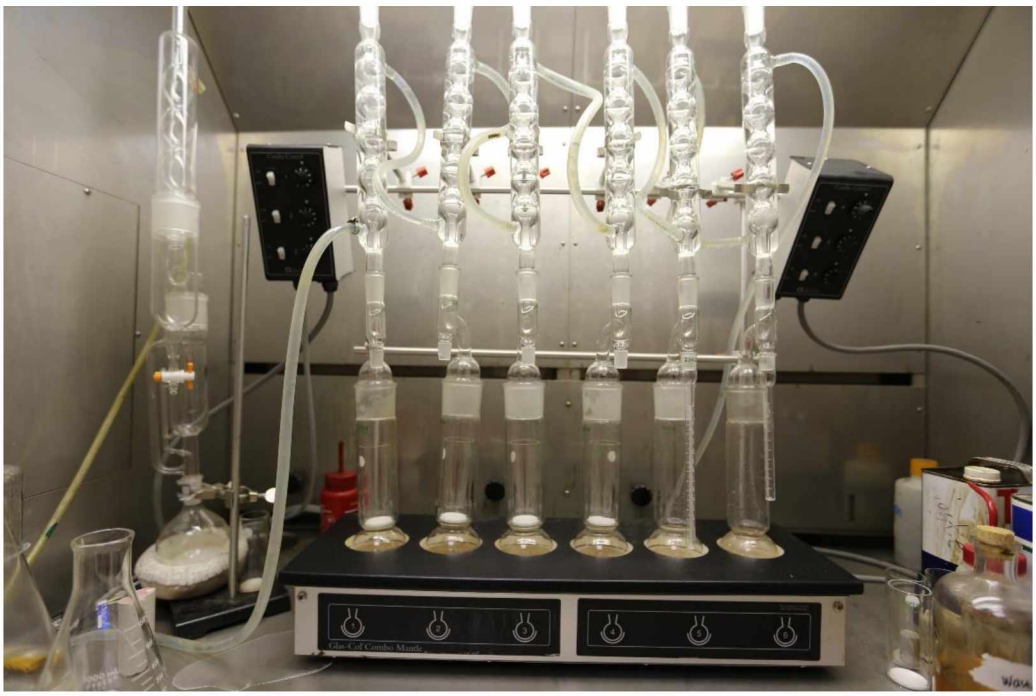

Figure 4.4 Dean-Stark Extraction System

4.2.4 Olympus Optical Microscope

The OLYMPUS series optical microscope system (see *Figure 4.5*) is employed to take a microgram of the emulsions, from which the emulsion type can be determined. With digital camera and imaging analysis software supplied by OLYMPUS, high quality photos of samples are captured with clear images of microstructures.

Figure 4.5 Olympus Optical Microscope

4.2.5 Cam-Plus Contact Angle Meter

The Cam-plus contact angle meter (see *Figure 4.6*) manufactured by Tantec is used to measure contact angle. The product is a benchtop optical device incorporating a projection screen with a protractor readout calibrated in two-degree increments. A droplet of testing liquid is placed on the tested surface by bringing the surface into contact with a droplet suspended from a needle of a syringe. For a water droplet, the equilibrium can be reached in seconds; for oil droplets, the

equilibrium can be achieved in approximately three minutes (once equilibrium has been reached the angle starts to recede). The image of the droplet is projected on the screen and the angle is measured. The recommended droplet diameter is 10 divisions on the screen. The half-angle measuring method is used to measure contact angle by taking direct angle measurement. The dial of the protractor is calibrated to display the contact angle.

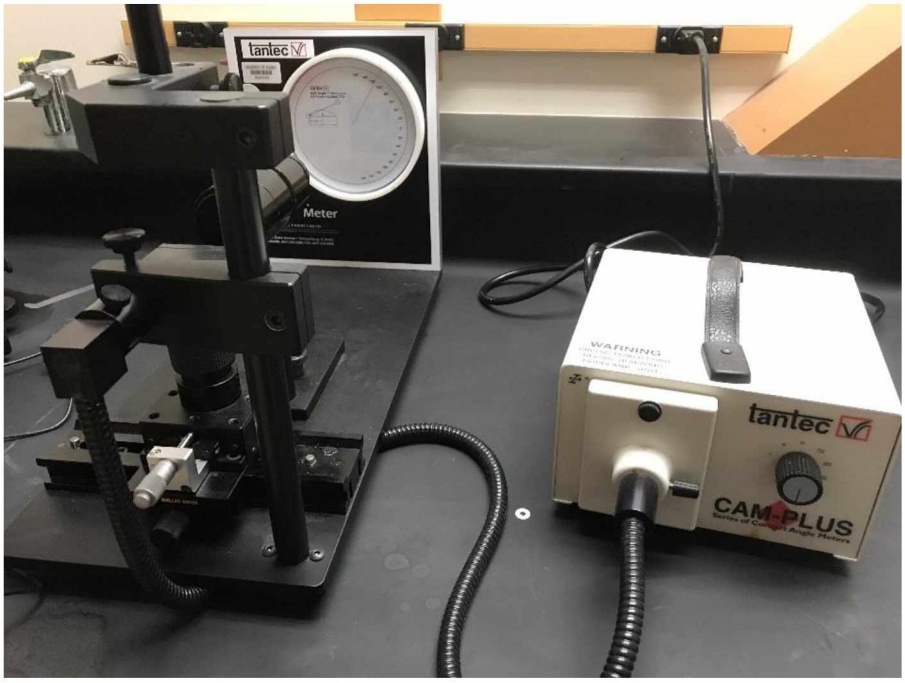

Figure 4.6 Cam-Plus Contact Angle Meter

4.2.6 Anton Paar Microviscometer and Density Meter

Anton Paar Microviscometers and Density Meters, shown in *Figure 4.7*, are employed to measure the viscosity and density of fluids. The microviscometer can provide high precision viscosity determination in a very wide viscosity and temperature range. The measurement principle of the microviscometer is the rolling ball (falling ball) principle, which can determine the viscosity of a sample by measuring the ball's rolling/falling time in a diagonally mounted

glass capillary. The density meter can show the results of samples and automatically convert the results into concentration, specific gravity, or other density-related units (including temperature compensation where necessary) using the built-in conversion tables and functions.

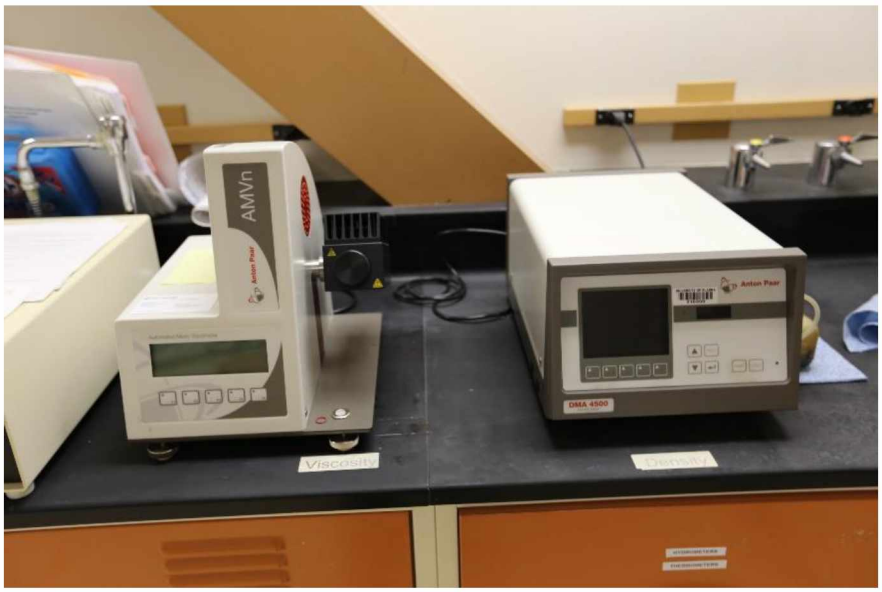

Figure 4.7 Anton Paar Microviscometer and Density Meters

4.2.7 Helium Porosimeter

A helium porosimeter, shown in *Figure 4.8*, is used to measure the porosity of the core plugs. A core plug is held in the chamber and compressive stress is applied. Grain volume, bulk volume, pore volume, grain density, and porosity of core plugs with diameters of 1 inch to 1.5 inches under ambient conditions are measured. The porosimeter functions up to a maximum pressure of 200 psi at room temperature.

Figure 4.8 Helium Porosimeter

4.2.8 Core Holder

The core holder is defined as having radial loading only. The core plug is held within a Viton sleeve by radial overburden pressure. Various core holders can accept core plugs of around 1.5 inches in diameter and 2 inches to 12 inches in length. For core plugs with undersized length, spacers can be supplied to occupy any unused space. The confining pressure of the core holders can be as high as 10,000 psi and at temperatures up to 177°C.

4.2.9 Accumulator

The accumulator could be used for various purposes, including displacement tests with displacement of fluids through core flooding, as well as being used as a recombination cell. The accumulator has a maximum working pressure of 10,000 psi at the maximum working temperature of 355°F (177°C), and a maximum volume of 1 liter. The movement of the

accumulator piston is controlled by an ISCO syringe pump. The ISCO pump is operated in constant flow rate mode during the core flooding procedure.

Other equipment included a vacuum, mixers, titration devices, filtration devices, and fluid flow lines.

4.3 Procedure

4.3.1 Preparation

(1) Core plugging

Core plugs were cut from the provided preserved core samples by using a drill press. The core plugs were examined visually and selected for displacement experiments. Compressed air was utilized as the cooling fluid during plugging, and this is to keep the original state of the core plugs.

(2) Water and oil property measurement

The Water and Environmental Research Center (WERC) helped to measure the salinity and compositions of the high salinity water and LSW. Then, 0.336 grams of soda ash per liter of water was added to the LSW to remove the divalent ions to make softened LSW. Since the salinity changed little, no further dilution with deionized water was needed for the softened LSW. An Anton-Paar Density Meter and Microviscometer was used to measure the density and viscosity of the provided oil sample, high salinity water, LSW, and the softened LSW.

4.3.2 Core Flooding Experiment Procedure

The fresh-state core plugs cut from the preserved core samples were flooded with the high salinity water, LSW, and softened LSW, successively, and the residual oil saturation after each flooding was determined based on material balance. The detailed procedure is described as follows:

(1) Purged all the lines entirely to make sure that there was no air in the system. The presence of air in the system would have amplified the fluctuations in pressure measurement;

(2) Filled the high salinity water, LSW, and softened LSW into accumulators A, B, and C, respectively. These fluids were used to flood the core plug sequentially;

(3) Weighed the core plug and recorded the weight as $W_{original}$ before loading the core plug into the core holder;

(4) Connected all the lines and fittings tightly to make sure there were no leaks;

(5) No back pressure was applied, and the temperature was set to be room temperature since the crude oil is dead oil;

(6) Applied 500 psi net confining pressure to the core plug. The core plug was now ready for the displacement experiment;

(7) Connected accumulator A (high salinity water) to the core holder. The pump was set at a constant flow rate to pump the high salinity water into the core holder in order to displace the oil in the core plug. During the displacement, the software was used to monitor and record the experimental data. Specifically, the overburden pressure needed to be tuned in real time to make sure the overburden pressure was always 500 psi higher than the inlet pressure so that the net confining pressure was always 500 psi. After injecting about 10

pore volumes (PV) of high salinity water, the cumulative oil production ($COP_{high\text{-}salinity\text{-}water}$) was recorded, and the injection was changed to LSW;

(8) Disconnected accumulator A (high salinity water) from the core holder, and connected accumulator B (LSW) to the core holder. Then continued to flood the core plug using LSW at a constant injection rate, while experimental parameters were monitored and recorded. After injecting about 10 PV of water, the new cumulative oil production ($COP_{low\text{-}salinity\text{-}water}$) was recorded, and the injection was changed to softened LSW;

(9) Disconnected accumulator B (LSW) from the core holder, and connected accumulator C (softened LSW) to the core holder. Then continued to flood the core plug using softened LSW at the constant injection rate, while the experimental parameters were monitored and recorded. After injecting about 10 PV of softened LSW, the cumulative oil production ($COP_{softened\text{-}water}$) was recorded;

(10) Stopped injection and released the pressures in the system; removed the core plug from the core holder and weighed, which is denoted as $W_{flooded}$;

(11) Cleaned the flooded core plug completely using the core cleaning system, while the water volume cleaned from the plug was recorded as $V_{w\text{-}cleaned}$;

(12) Dried the core plug completely, and weighed, which is denoted as W_{dry};

(13) Determined the core plug's porosity;

(14) Measured the produced oil density as $\rho_{original\text{-}oil}$;

(15) Calculated the original oil saturation, S_{oi}, and residual oil saturation after each flooding: The volume of water ($V_{w\text{-}cleaned}$) cleaned out from the plug had to be converted to an equivalent brine volume (V_{FW}) using a salt correction factor, SCF, since water collected in the Dean-Stark sidearm was distilled water, not brine, so,

$$V_{FW} = V_{w\text{-}cleaned} \times SCF \quad (1)$$

where

$$SCF = \frac{\rho_w}{\rho_{FW}} \times \frac{100}{100 - W\%salt} \quad (2)$$

where ρ_{FW} was the density of the softened LSW and W% salt was the weight percent of salt in the softened LSW.

The residual oil volume after displacement of softened LSW, $V_{oil\text{-}softened}$, was,

$$V_{oil-softened} = \frac{W_{flooded} - W_{dry} - V_{FW} \times \rho_{FW}}{\rho_{original-oil}} \quad (3)$$

Therefore, the residual oil saturation after softened LSW displacement was,

$$S_{or-softened} = \frac{V_{oil-softened}}{V_P} \quad (4)$$

where V_P was the pore volume.

The original oil saturation was calculated as,

$$S_{oi} = \frac{V_{oil-softened} + COP_{softened-water}}{V_P} \quad (5)$$

The residual oil saturation after high salinity water displacement was calculated as,

$$S_{or-high-salinity-water} = \frac{V_{oil-softened} + COP_{softened-water} - COP_{high-salinity-water}}{V_P} \quad (6)$$

The residual oil saturation after LSW displacement was calculated as,

$$S_{or-low-salinity-water} = \frac{V_{oil-softened} + COP_{softened-water} - COP_{low-salinity-water}}{V_P} \quad (7)$$

4.3.3 Relative Permeability Measurement Procedure

The unsteady-state experimental method was employed to measure the water-oil relative permeabilities for high salinity water and LSW, respectively, using restored state core plugs:

(1) Before any tests, the core plugs were cleaned thoroughly by using the core cleaning system, and dried completely;

(2) Vacuumed the dried core plug, then saturated it with high salinity water thoroughly, and measured its weight and recorded it as $W_{re\text{-}water}$. The saturated water volume was calculated as,

$$V_{re-water} = \frac{W_{re-water} - W_{dry}}{\rho_{high-salinity-water}} \quad (8)$$

(3) Purged all the lines entirely to make sure that there was no air in the system. Loaded the water-saturated core plug into the core holder. Connected all the lines and fittings, and applied a net confining pressure of 500 psi;

(4) Injected the high salinity water into the core plug at different volume flow rates to measure the absolute permeability of the core plug;

(5) Injected the provided crude oil at a low rate of 0.1 cc/minute into the brine-saturated core plug until no more brine was produced;

(6) Read and recorded the cumulative water production as $CWP_{re\text{-}water}$, and the initial/critical water saturation was calculated as,

$$S_{re-wi} = \frac{V_{re-water} - CWP_{re-water}}{V_P} \quad (9)$$

$$S_{re-oi} = 1 - S_{re-wi} \quad (10)$$

(7) The oil-saturated core plug was aged in oil for three weeks;

(8) Injected the provided crude oil into the aged core plug at different rates, and their corresponding pressure differences across the core plug were recorded; the oil effective permeability, $k_{eff,oil}$, at critical water saturation, S_{wi}, was determined using Darcy's Law. During injection, the overburden pressure was monitored and tuned in real time to make sure the net confining pressure of the core was 500 psi;

(9) Injected the high salinity water at a constant volume rate, $V_{inj\text{-}high\text{-}salinity\text{-}water}$, to displace the oil in the core plug, and the injection rate satisfied the following relationship (Rapoport and Leas 1953; Skauge et al. 2001) to minimize the capillary end effect:

$$L \times \mu_w \times v_w \geq 1 \quad (11)$$

where L was the length of the core, cm, μ_w was the viscosity of the injected water at experimental conditions, cP, and v_w was the flow velocity, mL/min. Cumulative oil production, cumulative water production, and pressure drop were monitored and recorded against time. In particular, the water breakthrough time needed to be monitored and recorded carefully;

(10) Continued the water flooding until pressure drop was stable;

(11) Injected the high salinity water into the core plug at different rates, and their corresponding pressure drops across the core plug were recorded; the water effective permeability, $k_{eff,water}$, at residual oil saturation, S_{or}, was determined by using Darcy's Law;

(12) Stopped injection, released all the pressures in the system, removed the core plug from the core holder, and recorded its weight as $W_{kr\text{-}high\text{-}salinity\text{-}water}$;

(13) Cleaned the core plug using the core cleaning system, and recorded the cleaned out water volume, $V_{kr\text{-}clean\text{-}out}$;

(14) Dried the core plug completely, and recorded its weight as $W_{kr\text{-}dry}$;

(15) Calculated the residual oil saturation, initial oil saturation, and initial water saturation according to material balance;

(16) Determined the relative permeabilities using the Johnson-Bossler-Naumann (JBN) method;

(17) Plotted the relative permeabilities versus water saturation;

(18) Repeated steps (1) to (17) to determine the relative permeabilities for LSW using the specified core plug.

4.3.4 Emulsification Test Procedure

The procedure of emulsification test is briefly described as follows:

(1) Mixed the provided crude oil with the LSW with a specific water-to-oil ratio;

(2) A homogenizer at 20,000 RPM for 4 minutes was used to generate the emulsion;

(3) The stability of the emulsion was investigated by using a simple bottle test;

(4) Emulsion type was determined by using an optical microscope, and finally

(5) The viscosity of the emulsion was measured using an Anton-Paar microviscometer.

4.3.5 Contact Angle Measurement Procedure

The contact angles between the crude oil and reservoir rock in the presence of high salinity water and LSW were respectively measured by a Tantec Cam-plus contact angle meter, and the procedure is described as follows:

(1) Core chip was cut from the preserved core, and the core chip dimensions were approximately 2 cm by 4 cm and 1 cm thickness;

(2) Core chip contact surface was polished carefully to make it flat and smooth;

(3) The core chip was then soaked in the high salinity water for at least 24 hours before the corresponding measurement;

(4) Filled the syringe with provided crude oil;

(5) Put the soaked core chip into a rectangular optical cell that is filled with high salinity water and place the cell on the specimen holder;

(6) Rotated the knob of the syringe clockwise to release the desired amount of oil; make sure the oil droplet touches the core chip surface;

(7) Waited for the transfer of the crude oil droplet to complete;

(8) Adjusted the specimen holder to bring the image into focus if necessary;

(9) Adjusted the vertical alignment to tune the height of the core chip surface so that the image is aligned with the horizontal cross-line of the measurement gauge;

(10) Slide the round measuring screen on the vertical back panel of the meter until the vertical cross-line touches the left edge of the crude oil droplet;

(11) Rotated the clear protractor on the measuring screen until the protractor's line crosses the oil droplet's apex;

(12) Read the contact angle on the scale to the nearest whole degree;

(13) Repeated steps (1) to (12) to measure contact angle between crude oil and reservoir rock in the presence of LSW.

5. Results and Discussion

5.1 Core Plug Properties

5.1.1 Core Plug Properties for Core Flooding Experiments

Preserved Core One (3,901 feet to 3,902 feet) was first cut, and four core plugs were obtained. Only one of the four core plugs passed initial visual inspection. *Figure 5.1* shows Preserved Core One with the bottom to the top of the core going from left to right. As can be seen, the plug cut from the lower part of the preserved core (Plug 1-1) was solid rock without any oil. The middle two plugs (Plug 1-2 and 1-3) were fractured during drilling due to their unconsolidated nature. Only the plug cut from the upper part (Plug 1-4) was complete, which was used for the first core flooding experiment. The core plug was 1.5 inches in diameter by 2.75 inches long, and its original weight before flooding was 154.272 grams. After the core flooding experiment, the porosity of the core plug 1-4 was determined to be 33.30%. The initial water saturation was 27.7%, and the initial oil saturation was 72.3%. The detailed properties are tabulated in *Table 5.1*.

Plug 1-1 Plug 1-2 Plug 1-3 Plug 1-4

Figure 5.1 Core Plugs from Preserved Core One

Table 5.1 Core Plug 1-4 Properties for the 1st Core Flooding Experiment

Length, inch	2.75
Diameter, inch	1.5
Pore Volume (PV), cm3	25.71
Porosity, %	33.30 (Average value)
Swi, frac	0.277
Soi, frac	0.723
Water Volume, mL	7.13
Oil Volume, mL	18.58
Original Weight, gram	154.272

Preserved Core Two was pre-marked with locations for each plug, and a total of five core plugs were cut. However, out of the five cuttings, only three core plugs passed initial visual inspection. One of the core plugs seemed to break apart in the cutting process completely and produced only oily unconsolidated sand in the bit and the drill cavity. The other non-viable case produced sand and fractured non-reservoir rock. Thus, three core plugs, as shown in *Figure 5.2*, were made ready to conduct the second core flooding experiment.

Core Plug 2-2 was first used to carry out the core flooding experiment. However, after several hours of displacement, it was found that only water was produced, which is not normal. The core flooding experiment was stopped, and when Core Plug 2-2 was taken out of the core holder, it was found that Core Plug 2-2 was fractured. Core Plug 2-3 was then used to conduct the core flooding experiments. Similarly, only water was produced after several hours' displacement. The core flooding experiment had to be stopped. When Core Plug 2-3 was taken out, the core plug was complete and not fractured. However, the surface around the core plug was found to be wet, so it was believed that water passed over the core plug in the space between the core plug and sleeve. The surface of Core Plug 2-3 was very coarse compared with the other two cores, so the sleeve might not have sealed around the core plug tightly enough. In the end, Core Plug 2-1 was used to conduct the core flooding experiment, and this time the displacement was successful. The dimensions of Core Plug 2-1 were 2.1 inches in length and 1.48 inches in diameter, and its original weight before flooding was 112.784 grams. After the core flooding experiment, the porosity was determined to be 33.14%. The initial water saturation was 22.0%, and the initial oil saturation was 78.0%. The detailed properties of core plug 2-1 are listed in *Table 5.2*.

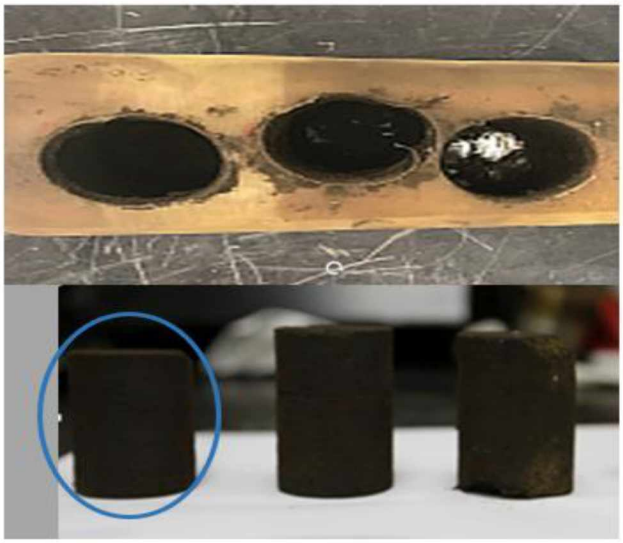

Figure 5.2 Core Plugs from Preserved Core Two

Table 5.2 Core Plug 2-1 Properties for the 2nd Core Flooding Experiment

Length, inch	2.1
Diameter, inch	1.48
Pore Volume (PV), cm3	19.61
Porosity, %	33.14
Swi, frac	0.220
Soi, frac	0.780
Water Volume, mL	4.31
Oil Volume, mL	15.30
Original Weight, gram	112.784

5.1.2 Core Plug Properties for Relative Permeability Measurements

Core plug 1-4 used for the first core flooding experiment was employed to conduct the first relative permeability measurement. The core plug 1-4 was cut due to some end chipping during the core flooding experiment, and the updated core plug was named core plug 1-4-1. The updated dimensions of the core plug 1-4-1 were 1.923 inches in length and 1.48 inches in diameter. The porosity was 35.99%.

Table 5.3 Core Plug 1-4-1 Properties for the 1st Relative Permeability Measurement

Length, inch	1.923
Diameter, inch	1.48
Pore Volume (PV), cm^3	19.50
Porosity, %	35.99

Another provided core plug, 9-7S, was employed to conduct the second and third relative permeability measurement. Core plug 9-7S was 1.75 inches in length and 1.508 inches in diameter. The pore volume of the core plug was 16.96 cm^3, so its porosity was 33.11%.

Table 5.4 Core Plug 9-7S Properties for the 2nd and 3rd Relative Permeability Measurements

Length, inch	1.75
Diameter, inch	1.508
Pore Volume (PV), cm3	16.96
Porosity, %	33.11

5.1.3 Core Plug Properties of Endpoint Tests

Core plug 9-7S was utilized to conduct endpoint tests first. Then, two Buff Berea core plugs, BB-1 and BB-2, were employed to test value of endpoint of k_{rw}. The detailed properties of BB-1 and BB-2 are described in *Tables 5.5* and *5.6*, respectively.

Table 5.5 Properties of Core Plug BB-1

Length, inch	3.911
Diameter, inch	1.494

Table 5.6 Properties of Core Plug BB-2

Length, inch	4.945
Diameter, inch	1.495

5.2 Water Sample Properties

The provided high salinity water and LSW were tested for their primary ion composition, pH, density, and salinity, and the test results are tabulated in *Table 5.7*. For provided high salinity water, only concentrations of Ca^{2+}, Mg^{2+}, pH, density, and salinity were tested. To deposit out divalent ions, soda ash (Na_2CO_3) was added to the LSW, which was to soften the LSW. Calcium and magnesium ions were expected to precipitate out from the LSW by the addition of soda ash. Based on the tested Ca^{2+} and Mg^{2+} concentrations in the LSW and theoretical calculations, 0.336 grams of soda ash per liter of water was needed to precipitate out the divalent ions. After the reaction of the water with the soda ash, the calculated new salinity of the softened LSW was 2,969 mg/L, which is close to the original salinity of LSW. The difference may occur because the amount of Na^+ that added into the provided high salinity water is higher than the value of

Ca^{2+} and Mg^{2+} that is precipitated from provided high salinity water during softening process. Since the salinity difference was small, no further dilution with deionized water was needed for the softened LSW. The required soda ash was added to the water sample and stirred using a magnetic stirring rod for approximately ten minutes. The water, which was initially clear, became opaque and milky white during mixing. Once the solution was fully mixed, it was filtered using a vacuum filter apparatus, as shown in *Figure 5.3*. The filtered water returned to a transparent state. The filtered water was collected and bottled. Also, the ion composition of the softened LSW was tested and tabulated in *Table 5.7*. The precipitate was collected on the filter. The filter was placed in a 50^{o}C drying oven to remove any remaining water. Once thoroughly dried, the weight of the precipitate was compared to the calculated expected value, and they are very close.

Table 5.7 Ion Composition for Water Samples

	Cation (mg/L)								Anion (mg/L)		PH	Density (g/cm3)	Salinity (mg/L)
Ions	Ca^{2+}	Fe^{3+}	Mg^{2+}	Mn	Na^{+}	K^{+}	Si	Ba^{2+}	Cl^{-}	Sulfate			
Provided High Salinity water	368		284								7.91	1.107	28,000
LSW	104	0.06	16.43	0.2	723.61	4.44	4	2.67	1,256	Not Detected	8.02	1.0	2,940
Softened LSW	8.66	0.03	15.99	0	1,314.7	5.26	3.69	0.57			8.77	1.0	2,969

Figure 5.3 Softened LSW Filtration

As can be seen from *Table 5.7*, the salinities of the LSW and softened LSW were significantly lower than the salinity of the high salinity water. By adding soda ash to the LSW, the LSW was softened. The Ca^{2+} ion concentration in the softened LSW was much lower than that in the LSW. However, the concentration of Mg^{2+} showed little change between the LSW and softened LSW, which indicated that soda ash may not be effective for precipitating the magnesium ions. The softened LSW had the highest pH at a value of 8.77, while the high salinity water had the lowest pH at a value of 7.91. The LSW and softened LSW had the same density of 1.0 g/cm^3, while the density of high salinity water was 10.7% higher at 1.107 g/cm^3.

5.3 Core Flooding Experiments

5.3.1 1st Core Flooding Experiment

At the beginning of the first core flooding experiment, the initially provided high salinity water (without any filtration) was injected. The injection rate was set at 0.25 mL/min. It was found that the injection pressure increased rapidly, so at a time of 81 minutes, the injection rate was reduced to 0.1 mL/min. However, the injection pressure continued to increase to an extremely high value, so water injection was stopped at the time of 110 minutes. At the time of 111 minutes, injection was restarted. This time, the high salinity water was filtered with standard filter paper as shown in *Figure 5.4*, and the injection rate was set at 0.25 mL/min, but the injection pressure again increased rapidly to a high value. The injection rate was reduced to 0.1 mL/min, 0.05 mL/min, and then finally to 0.02 mL/min, but the injection pressure continued to increase. Thus, the injection had to be stopped at a time of 183 minutes.

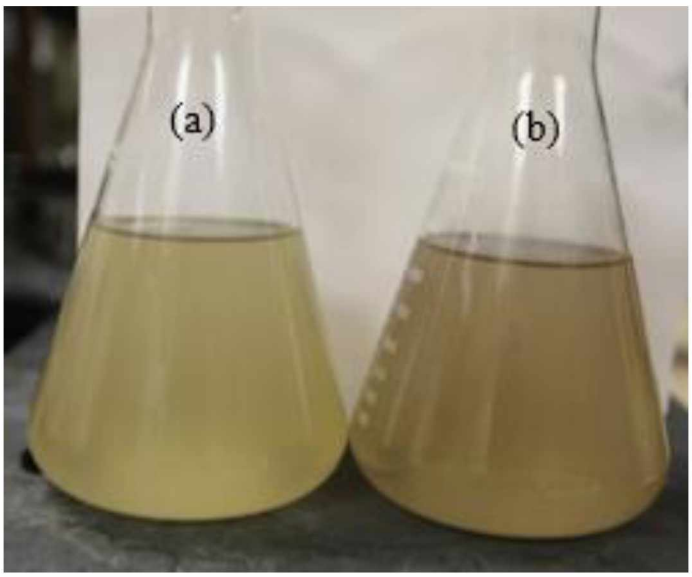

Figure 5.4 High Salinity Water Filtered with Standard Filter Paper (a) and Originally Provided High Salinity Water (b)

At the time of 184 minutes, the injection was restarted using high salinity water that was filtered with nano filter paper, as shown in *Figure 5.5*, at the injection rate of 0.1 mL/min. This time, the injection pressure was much lower. However, at a time of 568 minutes, the injection pressure exceeded the preset maximum injection pump pressure of 150 psi, so injection was stopped. At 909 minutes, injection was restarted at an injection rate of 0.1 mL/min (the injection was stopped between 569 and 909 minutes). Injection continued to the time of 2,837 minutes when the injection of high salinity water was finished.

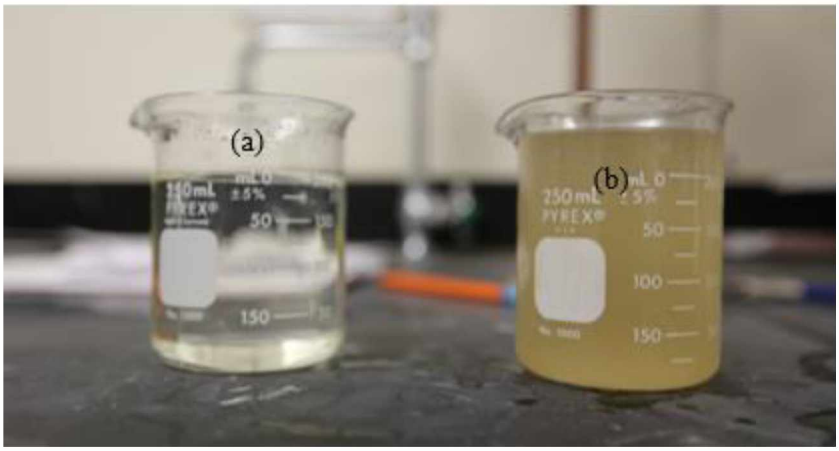

Figure 5.5 High Salinity Water Filtered with Nano Filter Paper (a) and High Salinity Water Filtered with Standard Filter Paper (b)

At the time of 2,838 minutes, the injection of LSW began. This injection phase continued to 6,335 minutes at an injection rate of 0.1 mL/min. During this phase, the injection was stopped and restarted several times as the injection pressure exceeded the preset maximum pump pressure on several occasions.

At 6,336 minutes, softened LSW injection started at an injection rate of 0.1 mL/min, which continued to the end of the experiment. During this phase, the injection was stopped and restarted several times since the injection pressure exceeded the preset maximum pump pressure on several occasions.

The injection pressure, injection rate, and total injection volume during the whole injection process was plotted and shown in *Figure 5.6*.

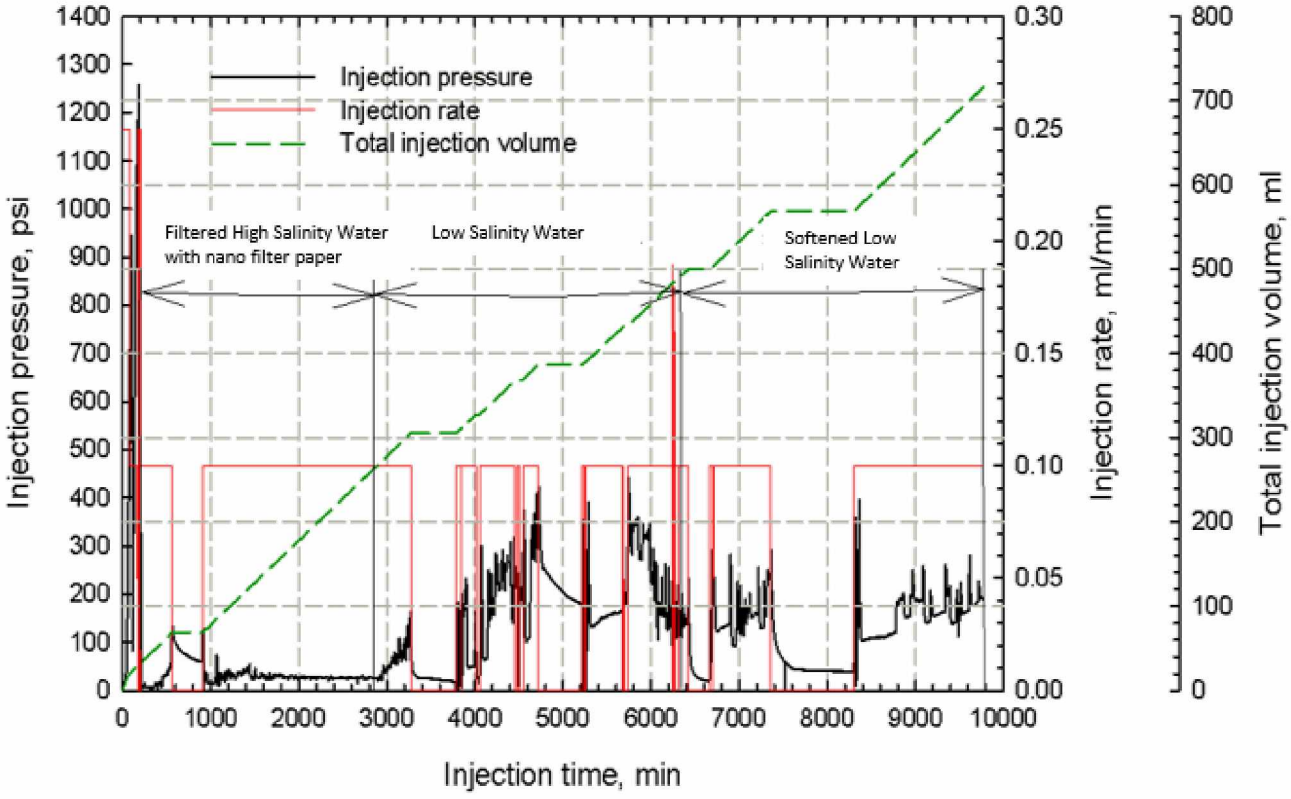

Figure 5.6 Injection Pressure, Injection Rate, and Total Injected Volume During Whole Injection Process of 1st Core Flooding Experiment

Figure 5.6 indicates that the initially provided high salinity water and high salinity water filtered with standard filter paper were much harder to inject, needing extremely high injection pressures. The high salinity water filtered with nano filter paper was much easier to inject, so all subsequent injected high salinity water was filtered using nano filters to remove impurities. The injection pressures of LSW and softened LSW were also higher than that of high salinity water filtered with nano filter paper and were associated with larger pressure fluctuations.

The cumulative oil production for the entire flooding process is shown in *Figure 5.7*. Injection of high salinity water produced a total of 7 mL of oil. An additional 0.99 mL of oil was produced by injecting LSW, and about 0.27±0.02 mL of oil was produced by injection of softened LSW. The water breakthrough time was found to occur between 82 and 110 minutes, which corresponds to an injected PV between 0.789 PV and 0.904 PV.

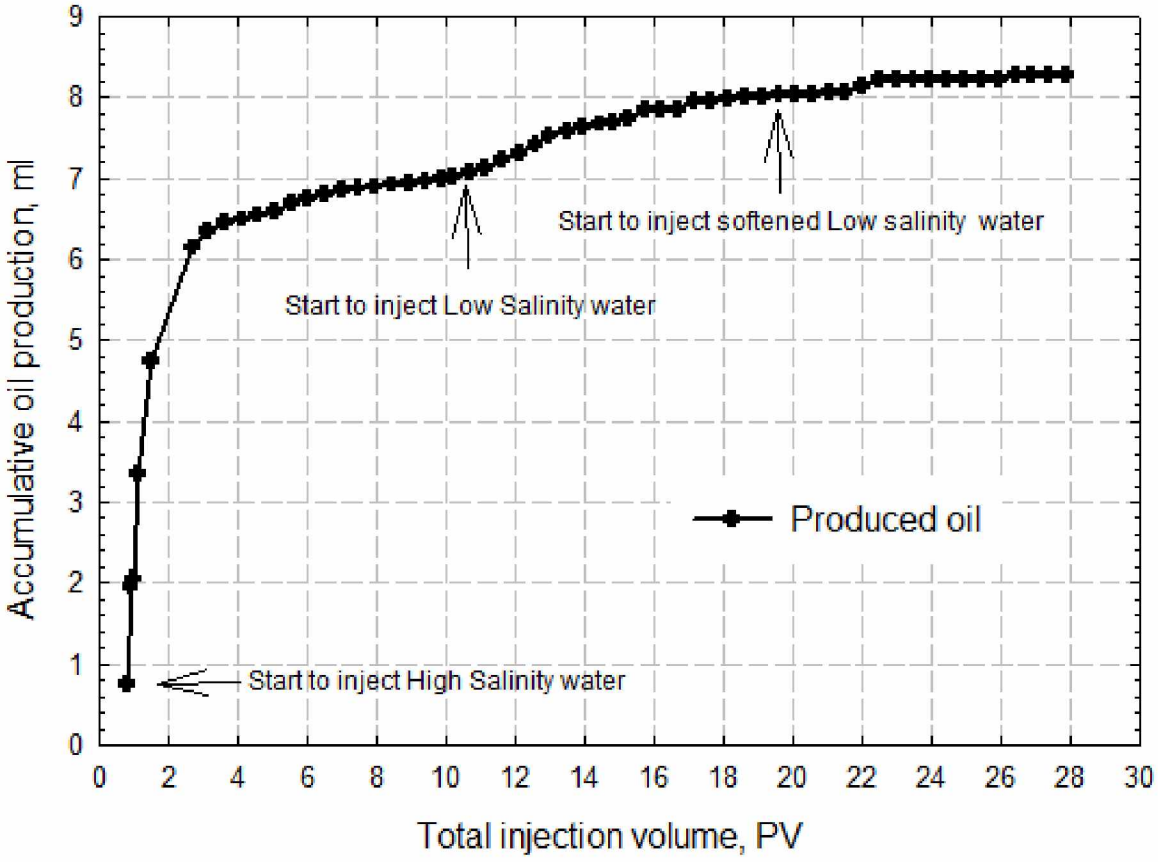

Figure 5.7 Accumulative Oil Production of 1st Core Flooding Experiment

The residual oil saturation after the softened LSW flooding was determined to be 40.14%. According to the inverse calculation, the residual oil saturation after LSW flooding was 41.19%, while the residual oil saturation after high salinity water flooding was 45.04%. Injection of LSW yielded 5.33% additional oil recovery over that of high salinity water. Injection of softened LSW had a slight incremental increase of 1.54% in oil recovery over that of LSW. The detailed results have been listed in *Table 5.8*.

Table 5.8 Oil Recovery Performance of 1st Core Flooding Experiment

	Residual Oil, mL	Residual Oil Saturation, %	Oil Recovery, %	Additional Oil Recovery, %
High Salinity Water	11.58	45.04	37.67	/
Low Salinity Water	10.59	41.19	43.00	5.33
Softened Low Salinity Water	10.32	40.14	44.45	1.54

5.3.2 2nd Core Flooding Experiment

The experiment process is similar to the 1st core flooding experiment, but core plug 2-1 was used. The high salinity water was first injected, and for this trial, the high salinity water was first nano filtered. After injection of 442 mL (22.54 PV) of high salinity water, the injection was changed to LSW. After injection of 430 mL (21.93 PV) of LSW, the injection was changed to softened LSW. The experiment was completed after injection of 430 mL (21.93 PV) of softened LSW. During the whole core flooding experiment process, the injection rate was set at 0.1 mL/min.

The injection pressure during the entire injection process was plotted and is shown in *Figure 5.8*. It can be seen from *Figure 5.8* that the injection pressure of LSW was lower than that of the high salinity water. Compared with the previous core flooding experiment, the injection pressures were much lower since the high salinity water was filtered using the nano filter paper. This water was much cleaner than that used in the initial stages of the 1st core flooding experiment. Also, the core used in the 2nd experiment was shorter than that used in the 1st experiment. Besides these

known factors, the permeability of the second core might be higher than that used in the 1st experiment.

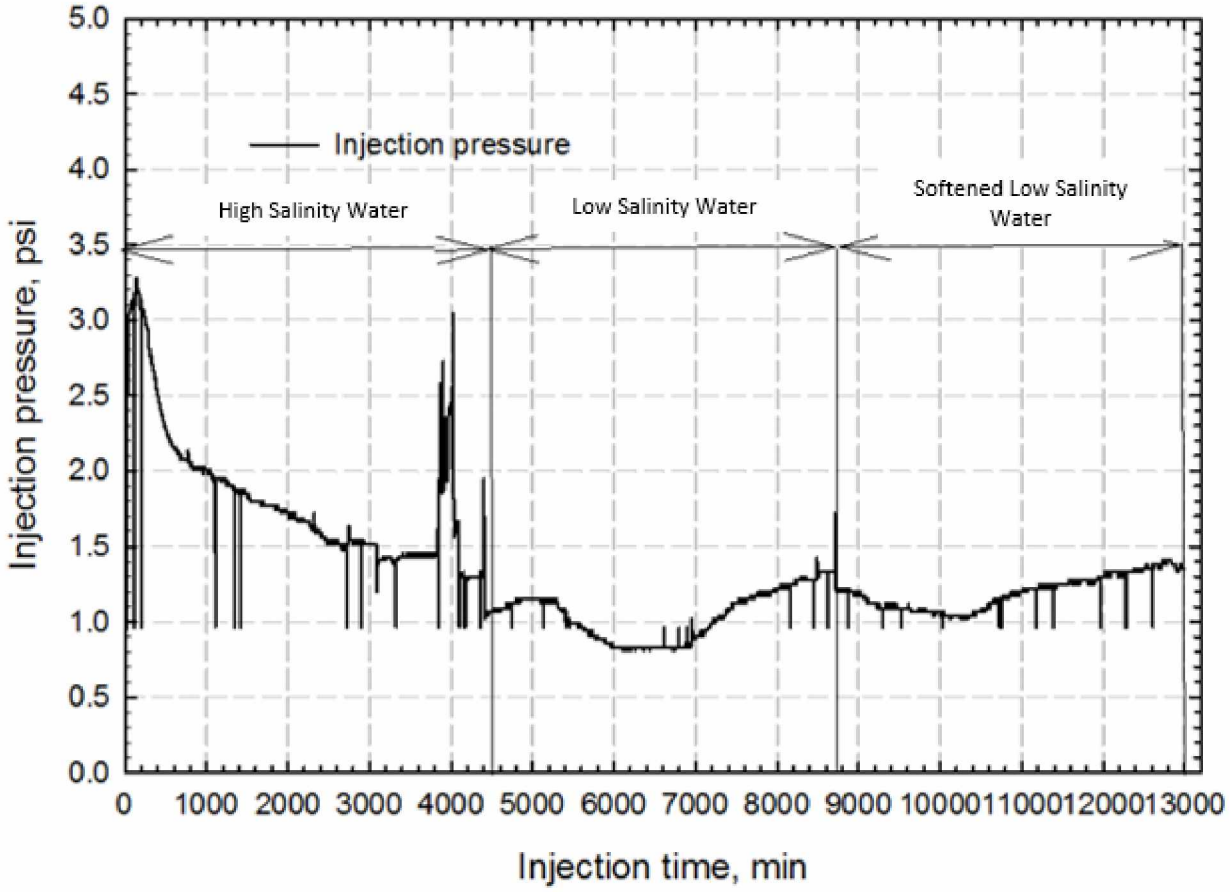

Figure 5.8 Injection Pressure of 2nd Core Flooding Experiment

The cumulative oil production for the 2nd core flooding experiment is shown in *Figure 5.9*. Injection of high salinity water produced a total of 4.99 mL of oil. An additional 1.07 mL of oil was produced by injecting LSW, and about 0.14±0.02 mL of oil was produced by injection of softened LSW.

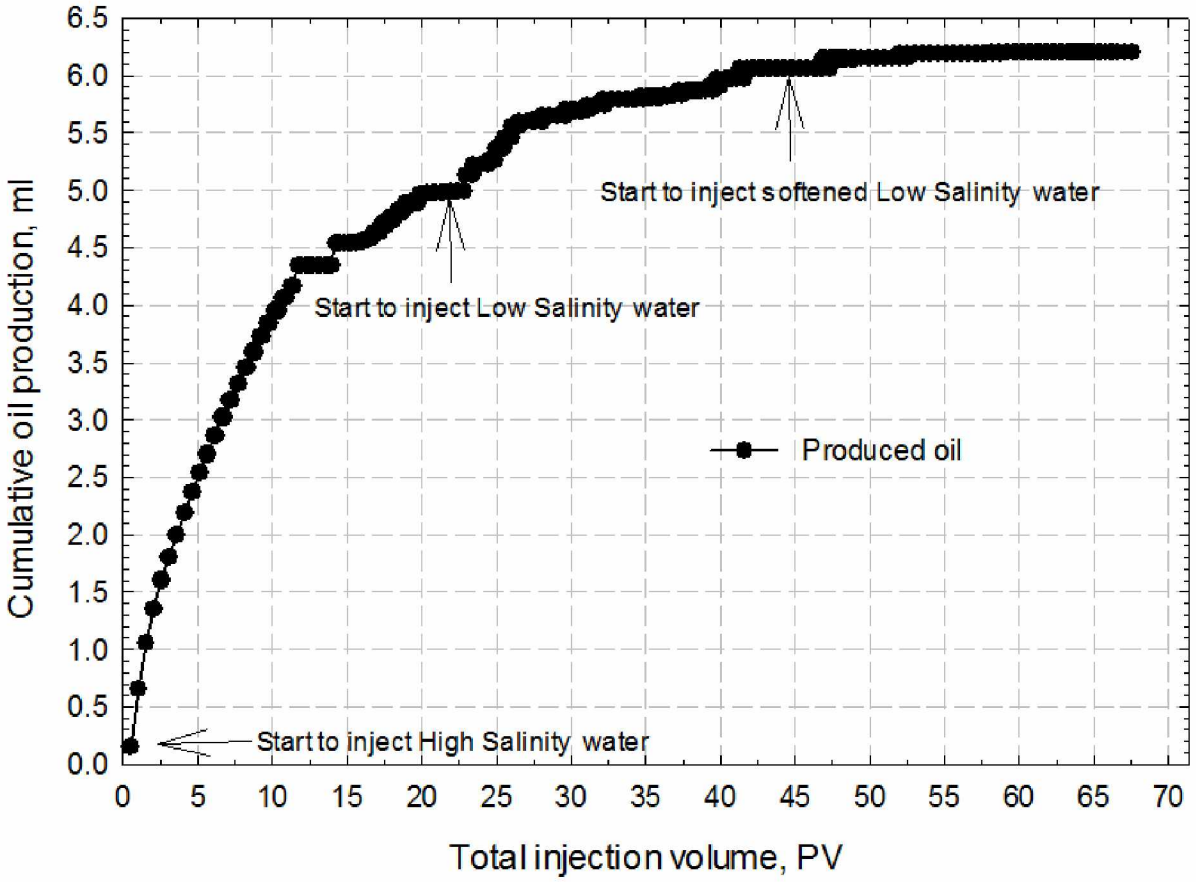

Figure 5.9 Cumulative Oil Production of 2nd Core Flooding Experiment

The residual oil saturation after softened LSW flooding was determined to be 46.40%. According to the back-calculation, the residual oil saturation after LSW flooding is 47.12%, while the residual oil saturation after high salinity water flooding is 52.58%. Injection of LSW yielded 7.00% additional oil recovery over that of high salinity water. Injection of softened LSW had a slight incremental increase of 0.91% in oil recovery over that of LSW. The detailed calculation results have been listed in *Table 5.9*.

Table 5.9 Oil Recovery Performance of 2nd Core Flooding Experiment

	Residual Oil, mL	Residual Oil Saturation, %	Oil Recovery, %	Additional Oil Recovery, %
High Salinity Water	10.31	52.58	32.61	/
Low Salinity Water	9.24	47.12	39.61	7.00
Softened Low Salinity Water	9.10	46.40	40.52	0.91

Both cumulative oil production curves generated based on the experimental results have the trend similar to that in Soraya et al.'s work (2009), which is that incremental oil recovery can be gained by injection of LSW. For all core flooding tests, production of fines was observed due to the core plugs' unconsolidated nature. As can be seen from the pressure curve in the first core flooding experiment, at the beginning, before high salinity water was filtered by nano filter paper, the injection pressure was extremely high and the experiment had to be stopped several times. This may be because the impurities and particles remaining in the high salinity water blocked the pore throats and permeable zones. Based on the pressure curve from the second core flooding experiment, the pressure decreased during the injection of high salinity water while both injection periods of LSW and softened LSW showed that the pressure increased after a critical point. It is clear to state that injection of LSW influences the flow resistance of injected water. With the LSW as the injected water, pressure drop increased after a critical point and peaked at a high value. By comparing results from previous work (Zhang et al. 2007), this may come from the blockage of porous media due to complex phenomena of oil/LSW/rock interaction that result in changes in redistribution and mobility of crude oil. In addition, as stated by Morrow and his

colleagues (Morrow 1975; Buckley et al. 1998; Tang and Morrow 1999), roughness and edges of rock surface, change in water composition and transient emulsion formation during LSWF, and fine migration resulting in formation damage can contribute to flow resistance (increased pressure drop) and remobilization of crude oil.

As calculated from oil production, LSWF can yield on average around 6% additional oil recovery. According to publications and principle from CNPC (China National Petroleum Corporation), a method that improves additional oil recovery over 4% can be considered as a successful way to produce oil. Therefore, injecting LSW to extract viscous oil can be regarded as a success.

5.4 Relative Permeabilities Measurements

5.4.1 1st Relative Permeability Measurement

The core plug, i.e., core plug 1-4, that was used in the first core flooding experiment was employed to conduct the 1st relative permeability measurement, and the relative permeabilities of high salinity water were measured. As it had been discussed above, the core plug was cut due to some end chipping during the first core flooding experiment (after cutting, the core plug name is updated to core plug 1-4-1, whose properties are listed in *Table 5.3*). After saturation with high salinity water, the absolute permeability of the core plug 1-4-1 was determined to be 147.9 mD, which was selected to be base permeability.

Provided oil was then injected at 0.1 mL/min to obtain initial oil saturation. The initial oil saturation was determined to be 60.65%, and the initial water saturation was 39.35%. The

effective oil permeability at initial water saturation was determined to be 77.8 mD. The detailed core plug 1-4-1 parameters are shown in *Table 5.10*.

Table 5.10 Core Plug 1-4-1 Parameters Tested from 1st Relative Permeability Measurement

Absolute Water Permeability, mD	147.9
Effective Oil Permeability at Initial Water Saturation, mD	77.8
S_{wi}, frac	0.3935
S_{oi}, frac	0.6065
Water Volume, mL	7.67
Oil Volume, mL	11.83

The residual oil saturation after the unsteady-state displacement experiment where the injection rate of high salinity water was fixed at 1 mL/min was determined to be 35.53%. The effective water permeability at residual oil saturation was determined to be 13.013 mD (average value of different injection rates). The detailed results are shown in *Table 5.11*.

Table 5.11 Results of the First Relative Permeability Measurement

Effective Water Permeability at Residual Oil Saturation, mD	13.013 (Average value)
S_{or}, frac	0.3552
S_w, frac	0.6448
Endpoint of k_{rw}	0.0879

The recorded pressure drop and cumulative oil production have been described in *Figure 5.10*.

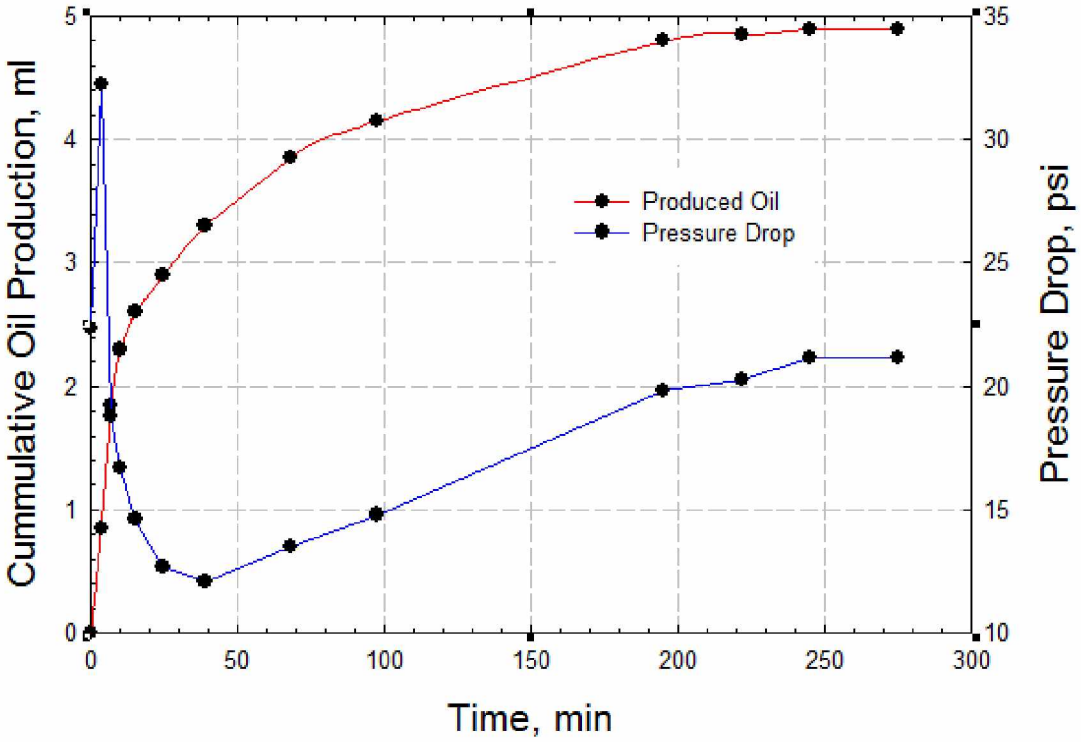

Figure 5.10 Pressure Drop and Cumulative Oil Production for the 1st Relative Permeability Measurement

Apparently, at the later period of the displacement experiment, between 50 minutes to the end of the test, the pressure drop continued to increase. According to the recorded cumulative oil production and pressure drops, the relative permeabilities of the high salinity water were calculated by using the JBN method. Results are shown in *Figure 5.11*.

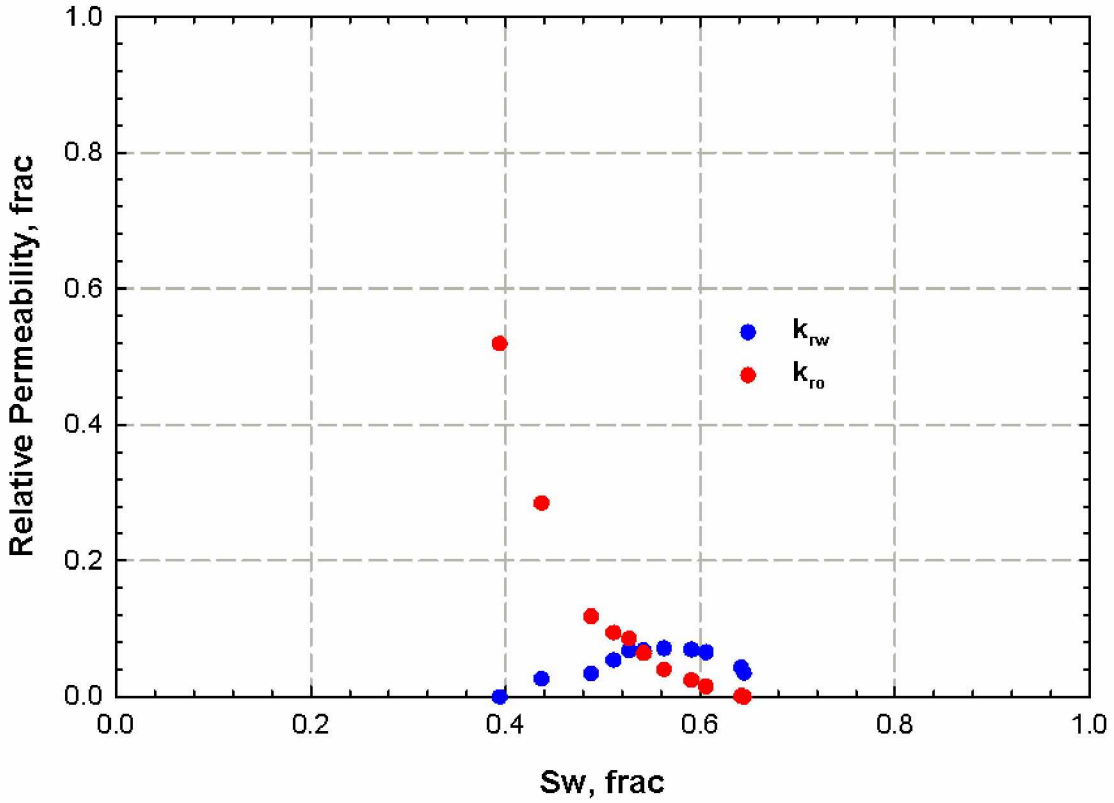

Figure 5.11 Relative Permeability Curves of High Salinity Water for the 1st Relative Permeability Measurement Where Injection Rate Was Fixed at 1 mL/min

5.4.2 2nd Relative Permeability Measurement

The provided core plug, 9-7S, was employed to conduct the 2nd relative permeability measurement, and the relative permeabilities of high salinity water were measured again. After saturation with high salinity water, the absolute permeability of the core plug was determined to be 327.7 mD, which was selected to be base permeability.

Then, the provided oil was injected at 0.1 mL/min to obtain initial oil saturation. The initial oil saturation was determined to be 51.59%, and the initial water saturation was 48.41%. The

effective oil permeability at initial water saturation was determined to be 69.4 mD. The parameters are shown in *Table 5.12*.

Table 5.12 Core Plug 9-7S Parameters Tested from 2nd Relative Permeability Measurement

Absolute Water Permeability, mD	327.7
Effective Oil Permeability at Initial Water Saturation, mD	69.4
S_{wi}, frac	0.4841
S_{oi}, frac	0.5159
Water Volume, mL	8.21
Oil Volume, mL	8.75

The residual oil saturation after the unsteady-state displacement experiment where the injection rate of high salinity water was fixed at 2 mL/min was determined to be 21.24%. The effective water permeability at residual oil saturation was determined to be 5.87 mD (average value of different injection rates). The results are shown in *Table 5.13*.

Table 5.13 Results of the 2nd Relative Permeability Measurement

Effective Water Permeability at Residual Oil Saturation, mD	5.87 (Average value)
S_{or}, frac	0.2124
S_w, frac	0.7876
Endpoint of k_{rw}	0.0179

The recorded pressure drop and cumulative oil production have been described in *Figure 5.12*.

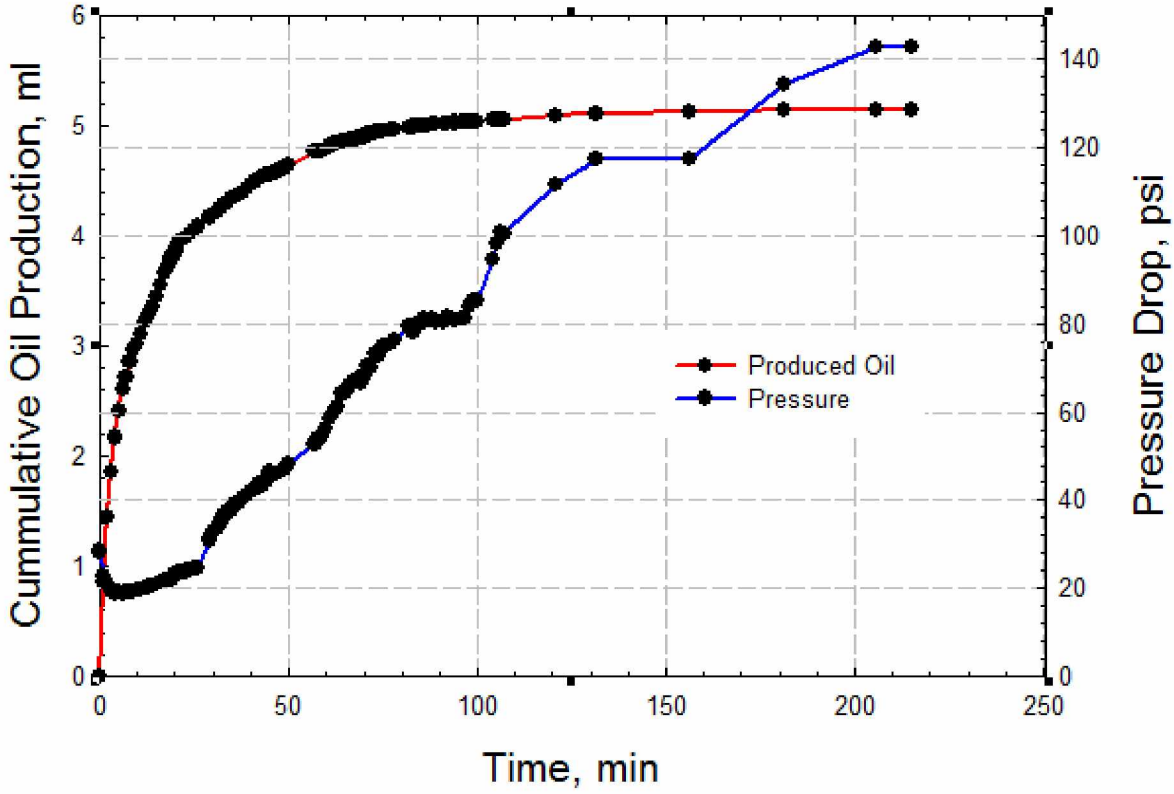

Figure 5.12 Pressure Drop and Cumulative Oil Production for the 2nd Relative Permeability Measurement

Starting at a time of 10 minutes past the start of displacement, the pressure drop began to increase and plateaued at 142 psi. According to the recorded cumulative oil production and pressure drop, the relative permeabilities of high salinity water were calculated by using the JBN method and are shown in *Figure 5.13*.

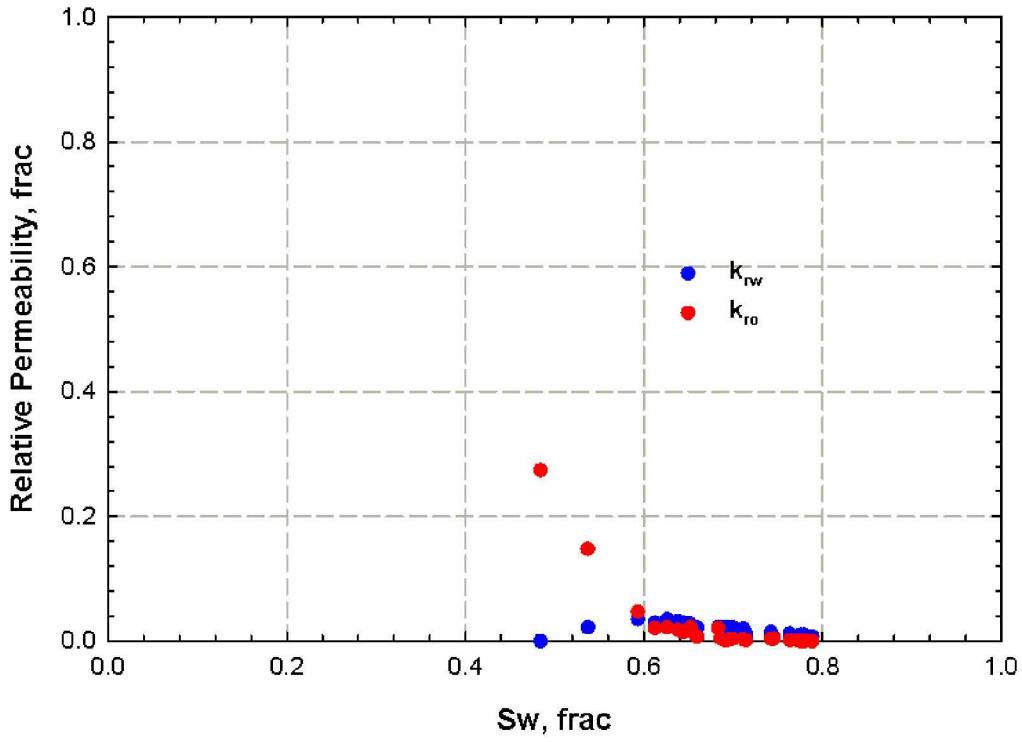

Figure 5.13 Relative Permeability Curves of High Salinity Water for the 2nd Relative Permeability Measurement Where Injection Rate Was Fixed at 2 mL/min

5.4.3 3rd Relative Permeability Measurement

In the third relative permeability measurement, relative permeabilities of LSW were measured, and core plug 9-7S was used to conduct the unsteady-state displacement experiment. After measuring the high salinity water relative permeabilities in subsection **5.4.2**, the provided core plug, 9-7S, was re-saturated with provided crude oil directly without cleaning. It is believed that this way can help retain the core plug's properties, especially the original wettability. The initial oil saturation was determined to be 51.01%, and the initial water saturation was 48.99%. The effective oil permeability at initial water saturation was determined to be 108.8 mD when the

injection rate was increased in sequence and 117.2 mD when the injection rate was reduced in sequence. These results are shown in *Table 5.14*.

Table 5.14 Core Plug 9-7S Parameter Tested from 3rd Relative Permeability Measurement

Effective Oil Permeability at Initial Water Saturation, mD	108.8 (increase injection rate); 117.2 (reduce injection rate)
S_{wi}, frac	0.4899
S_{oi}, frac	0.5101
Water Volume, mL	8.31
Oil Volume, mL	8.65

The residual oil saturation after the unsteady-state displacement experiment where the injection rate of LSW was fixed at 0.1 mL/min was determined to be 14.82%. The water effective permeability at residual oil saturation was determined to be 32.3 mD when the injection rate was increased in sequence and 34.5 mD when the injection rate was reduced in sequence. The detailed calculation results are shown in *Table 5.15*.

Table 5.15 Results of the 3rd Relative Permeability Measurement

Effective Water Permeability at Residual Oil Saturation, mD	32.3 (increase injection rate); 34.5 (reduce injection rate)
S_{or}, frac	0.1482
S_w, frac	0.8512
Endpoint of k_{rw}	0.102

The recorded pressure drop and cumulative oil production have been described in *Figure 5.14*.

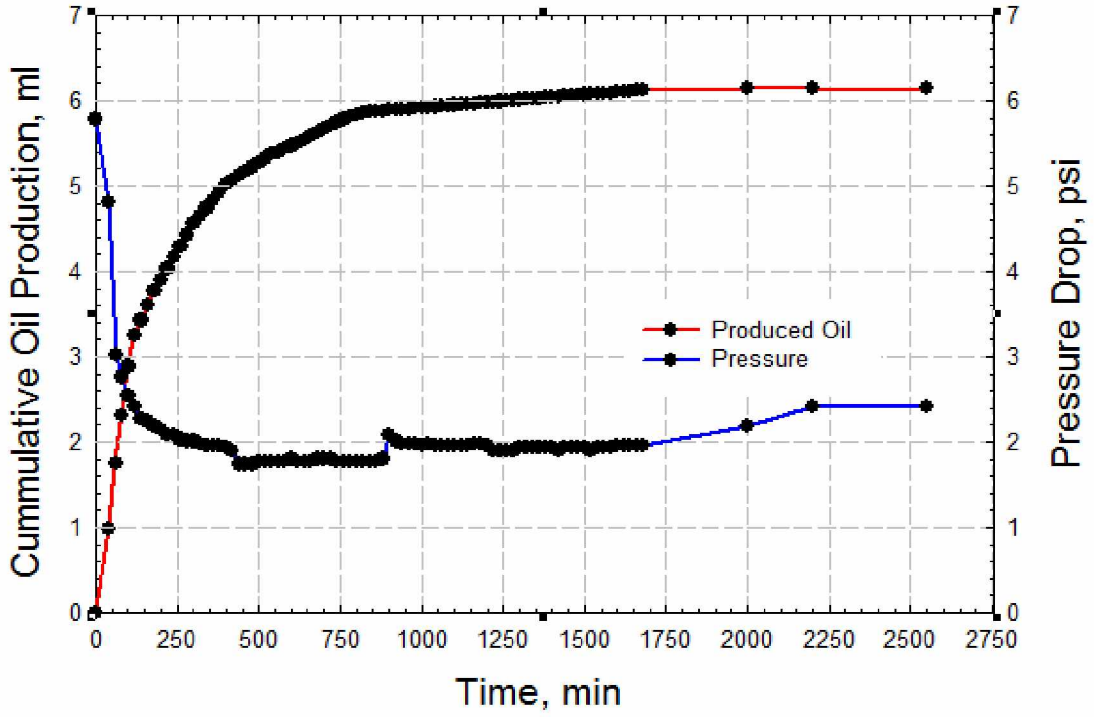

Figure 5.14 Pressure Drop and Cumulative Oil Production for the 3rd Relative Permeability Measurement

Apparently, in the latter part of the displacement starting from the time of 400 minutes, the pressure drop gradually increased up to 2.4 psi. According to the recorded cumulative oil production and pressure drop, the relative permeabilities of LSW were calculated by using the JBN method and are shown in *Figure 5.15*.

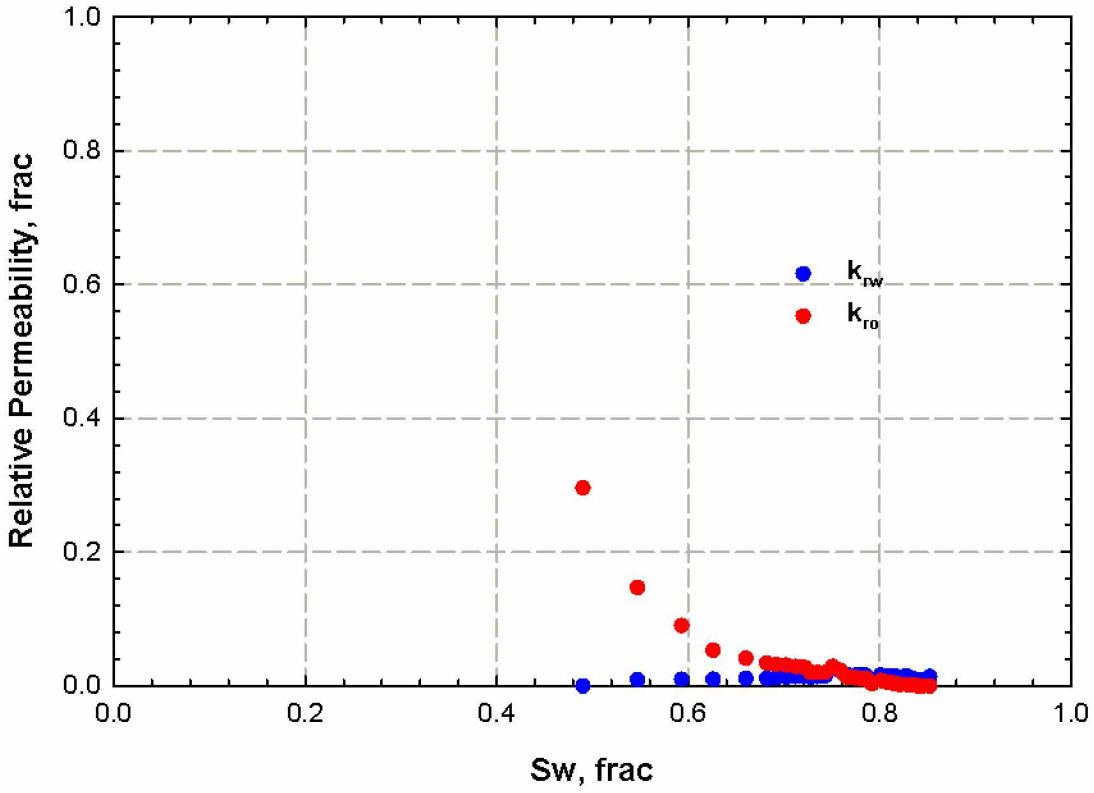

Figure 5.15 Relative Permeability Curves of LSW for the 3rd Relative Permeability Measurement Where Injection Rate Was Fixed at 0.1 mL/min

The unsteady-state displacement experiments showed the similar trend of pressure drop comparing to the trend of pressure drop from core flooding experiments. The pressure drop decreased at first, then gradually increased to a relative high value, which was different from the pressure drop trend in the conventional displacement experiment. This pressure drop trend is also reflected at water relative permeability curves, in which the value of k_{rw} peaked as the pressure drop reduced to the lowest value and the value of k_{rw} started to decrease while the pressure drop increased. By comparing the first and second relative permeability measurements, the pressure drop plateaued at a much higher value when the injection rate of LSW was higher. The endpoint of k_{rw} is influenced by the injection rate of water as well: the higher water injection rate resulted

in lower value of endpoint. Some researchers believe that relative permeability is independent of injection rate while some others report that relative permeability does change as flow rate changes (Torabzadey 1984; Heaviside et al. 1987; Akin and Demiral 1997). Sufi et al. (1982) found that water relative permeability curves increased with increasing injection rates until critical injection rate was reached where relative permeability curves were independent above the critical injection rate. However, compared with first and second relative permeability curves, the water relative permeability curve decreased with increasing the injection rate, indicating that during the relative permeability measurements the relative permeability curves has little effect on relative permeability. By comparing the water relative permeability curves from the three displacement experiments, the third water relative permeability curve (injected water is LSW) is more suppressed than the first two water relative permeability curves (injected water is high salinity water), which indicates that the wettability of rock surface changed towards more water-wet state during the injection of LSW. The wettability alteration is also interpreted by the intersection of the oil and water relative permeabilities (Morrow et al. 1973), which shifted to the right when the injected water is LSW compared with a period of high salinity water injection. One of the possible reasons for this unconventional pressure drop trend and unorthodox water relative permeability curve may be particle migration in the displacement experiment since the experimental core plugs are very unconsolidated and associated with high clay content. Fine migration, which reduces permeability and blocks pore throats or pore constructions resulting in formation damage, can be a significant problem when rock contains clays and naturally existing fines (Batycky et al. 1981). The other potential answer to this irregular pressure drop trend and unusual water relative permeability curve is in-situ emulsification during displacements and interactions between injected LSW/oil/rock.

5.5 k_{rw} Endpoint Tests

According to the calculated relative permeabilities from the above three experiments, it has been found that all the calculated values of endpoint of k_{rw} are lower than the expected typical value. Therefore, several additional experiments were designed and conducted to validate the measurement results. LSW was employed to test the values of endpoint of k_{rw}, but different core plugs and oil samples were used to conduct the tests. The base permeability is absolute water permeability.

5.5.1 Core Plug BB-1 Test (Saturated with Provided Oil)

The experimental procedure is the same as the previously described unsteady-state displacement experiment, but the core plug BB-1 and provided viscous oil were employed in the test. The absolute permeability of LSW was determined to be 338.3 mD when the injection rate was increased in sequence and 339.5 mD when the injection rate was reduced in sequence. The effective oil permeability at initial water saturation was determined to be 138.6 mD when the injection rate was increased in sequence and 137.4 mD when the injection rate was reduced in sequence. The water effective permeability of LSW at residual oil saturation was determined to be 28.6 mD when the injection rate was increased in sequence and 31.6 mD when the injection rate was reduced in sequence. The endpoint of k_{rw} was finally determined to be 0.0888. After the displacement experiment, the provided oil was re-injected into the core until no further water production was observed. Then, the effective oil permeability at initial water saturation was measured again. The oil effective permeability at initial water saturation was determined to be 136.5 mD when the injection rate was increased in sequence and 135.3 mD when the injection

rate was reduced in sequence. Therefore, the oil effective permeability could be recovered. The detailed results are shown in *Table 5.16*.

Table 5.16 Results of Core Plug BB-1 Test (Saturated with Provided Viscous Oil)

Absolute Water Permeability, mD	338.3 (increase injection rate); 339.5 (reduce injection rate)
Effective Oil Permeability at Initial Water Saturation, mD	138.6 (increase injection rate); 137.4 (reduce injection rate)
Effective Water Permeability at Residual Oil Saturation, mD	28.6 (increase injection rate); 31.6 (reduce injection rate)
Endpoint of k_{rw}	0.0888
Effective Oil Permeability at Initial Water Saturation, mD (Re-Saturated with Provided Oil)	136.5 (increase injection rate); 135.3 (reduce injection rate)

5.5.2 Core Plug BB-2 Test (Saturated with Light Oil)

The core plug BB-2 and the light oil whose API gravity is 37.5° were employed to conduct the experiment in this test. The absolute permeability of LSW was determined to be 401.7 mD when the injection rate was increased in sequence and 390.5 mD when the injection rate was reduced in sequence. The oil effective permeability at initial water saturation was determined to be 176.2 mD when the injection rate was increased in sequence and 183.8 mD when the injection rate was reduced in sequence. The effective water permeability of LSW at residual oil saturation was determined to be 56.7 mD when the injection rate was increased in sequence and 61.4 mD when the injection rate was reduced in sequence. Finally, the endpoint of k_{rw} at residual oil saturation was determined to be 0.149. The detailed results are shown in *Table 5.17*.

Table 5.17 Results of Core Plug BB-2 Test (Saturated with Light Oil)

Absolute Water Permeability, mD	401.7 (increase injection rate); 390.5 (reduce injection rate)
Effective Oil Permeability at Initial Water Saturation, mD	176.2 (increase injection rate); 183.8 (reduce injection rate)
Effective Water Permeability at Residual Oil Saturation, mD	56.7 (increase injection rate); 61.4 (reduce injection rate)
Endpoint of k_{rw}	0.149

5.5.3 Core Plug 9-7S 1st Test (Saturated with Light Oil)

The cleaned and dried 9-7S core plug was used to conduct the endpoint test, but the light oil whose API gravity is 37.5° was saturated first. The oil effective permeability at initial water saturation was determined to be 86.2 mD if the injection rate was increased in sequence and 90.0 mD if the injection rate was reduced in sequence. The effective water permeability of LSW at residual oil saturation was determined to be 47.2 mD when the injection rate was increased in sequence and 60.6 mD when the injection rate was reduced in sequence. The value of endpoint of k_{rw} was finally determined to be 0.164 (using water absolute permeability of 327.7 mD as the base permeability). The results were shown in *Table 5.18*.

Table 5.18 Results of Core Plug 9-7S 1st Test (Saturated with Light Oil)

Effective Oil Permeability at Initial Water Saturation, mD	86.2 (increase injection rate); 90 (reduce injection rate)
Effective Water Permeability at Residual Oil Saturation, mD	47.2 (increase injection rate); 60.6 (reduce injection rate)
Endpoint of k_{rw}	0.164

5.5.4 Core Plug 9-7S 2nd Test (Re-saturated with Provided Oil)

After the displacement experiment in **5.5.3**, the core plug 9-7S was re-saturated with provided viscous oil directly, and another unsteady-state displacement experiment was conducted. The oil effective permeability at initial water saturation was determined to be 64.3 mD when the injection rate was increased in sequence and 65.6 mD if the injection rate was reduced in sequence. The effective water permeability of LSW at residual oil saturation was determined to be 39.5 mD if the injection rate was increased in sequence and 41.7 mD if the injection rate was reduced in sequence. The endpoint of k_{rw} was determined to be 0.124. The detailed results are shown in *Table 5.19*.

Table 5.19 Results of Core Plug 9-7S 2nd Test (Saturated with Provided Oil)

Effective Oil Permeability at Initial Water Saturation, mD	64.3 (increase injection rate); 65.6 (reduce injection rate)
Effective Water Permeability at Residual Oil Saturation, mD	39.5 (increase injection rate); 41.7 (reduce injection rate)
Endpoint of k_{rw}	0.124

By comparing the results in *Tables 5.16* and *5.17*, it can be found that, with similar core properties and water properties, the value of endpoint of k_{rw} in the presence of light oil is reasonable, but the value of endpoint of k_{rw} in the presence of provided viscous oil is much lower. This indicates some unusual or complex interaction between the LSW and provided viscous oil. By comparing the results in *Tables 5.15* and *5.18*, the value of endpoint of k_{rw} in the presence of light oil is higher than the value in the presence of provided viscous oil, further implying complex reactions between the LSW and provided viscous oil. By comparing the results in

Tables 5.18 and *5.19*, the value of endpoint of k_{rw} was reduced by changing the oil to the provided viscous oil. What is more, after the displacement experiment and measuring the endpoint for the core plug BB-1, the provided oil was re-injected into the core plug until no more water was produced. Also, the effective oil permeability was recovered, which means that fine migration may not be the reason for abnormal value of endpoint of k_{rw}.

5.6 Emulsion Examination

According to the experimental validation results in **5.5**, the lower values of the endpoint of k_{rw} might be a result of the interactions between the water, crude oil, and reservoir rock. Therefore, an investigation of the emulsification of the crude oil and injection water was desirable. In this study, the emulsification between the provided viscous oil and LSW was investigated, including emulsion type, viscosity, and stability. Emulsification phenomenon of three water-oil ratios of 20:80, 50:50, and 80:20 was investigated. Emulsions were prepared by adding the provided crude oil to LSW to attain the particular water-oil ratio. Then, a homogenizer at 22,000 RPM set for 4 minutes was used to generate the emulsion. In all cases, both the oil sample and LSW samples were equilibrated at room temperature and pressure before mixing. The emulsion samples were kept at the same temperature for at least 24 hours before any photos of emulsion droplets were taken.

5.6.1 Emulsion Stability

Stability analysis for emulsions was performed using simple bottle tests as shown in *Figures 5.16-5.18*.

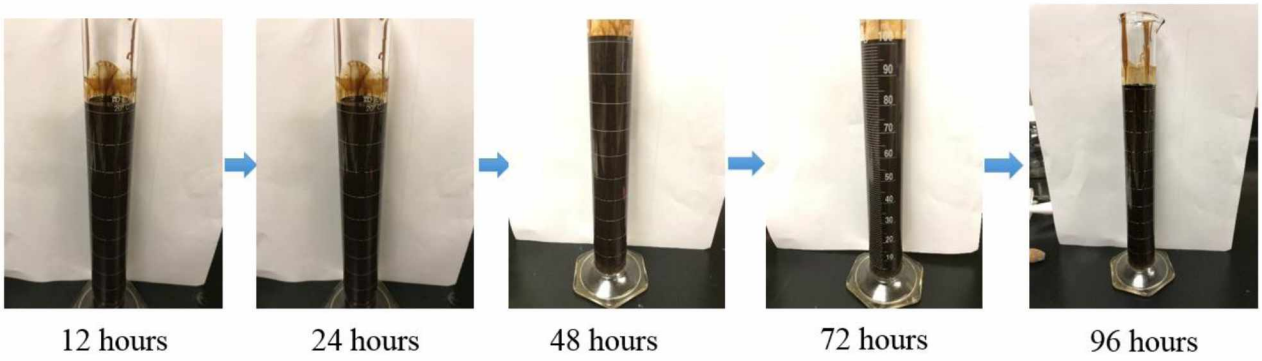

Figure 5.16 Emulsion Stability (Water-Oil Ratio of 20:80)

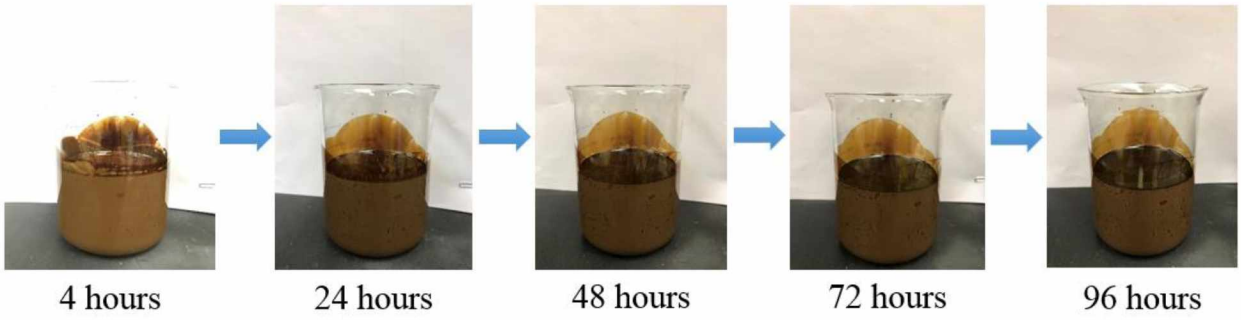

Figure 5.17 Emulsion Stability (Water-Oil Ratio of 50:50)

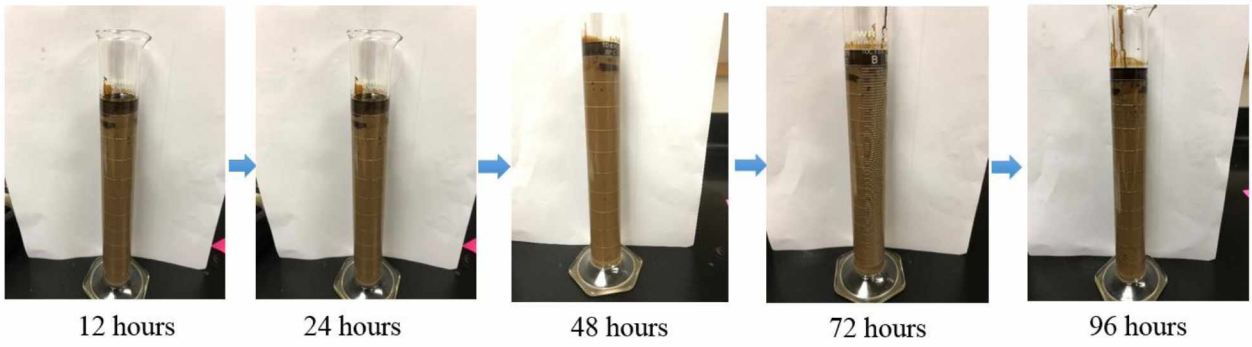

Figure 5.18 Emulsion Stability (Water-Oil Ratio of 80:20)

The figures shown above demonstrate the phases separating after mixing the provided oil and LSW. As can be seen, after a long time, for all three water-oil ratios, only a small amount of crude oil separated out, and no visible water separation was observed, indicating the generated emulsions were stable.

5.6.2 Emulsion Type

An optical microscope was utilized to take pictures of the emulsions. The optical microscopic images were taken after the emulsions were stable, as shown in *Figures 5.19-5.21*.

Figure 5.19 Optical Microscopic Image of the W/O Emulsion (Water-Oil Ratio of 20:80)

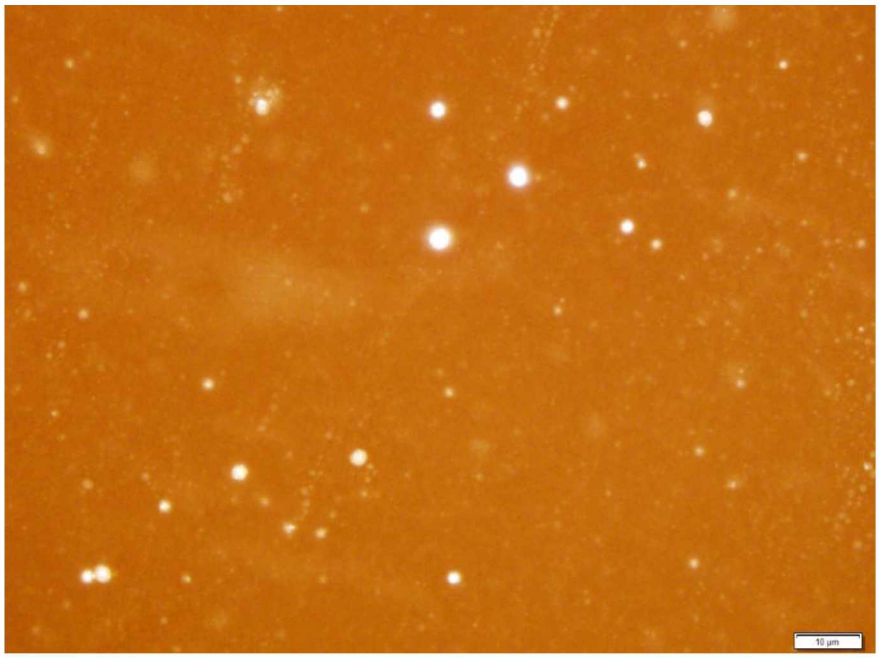

Figure 5.20 Optical Microscopic Image of the W/O Emulsion (Water-Oil Ratio of 50:50)

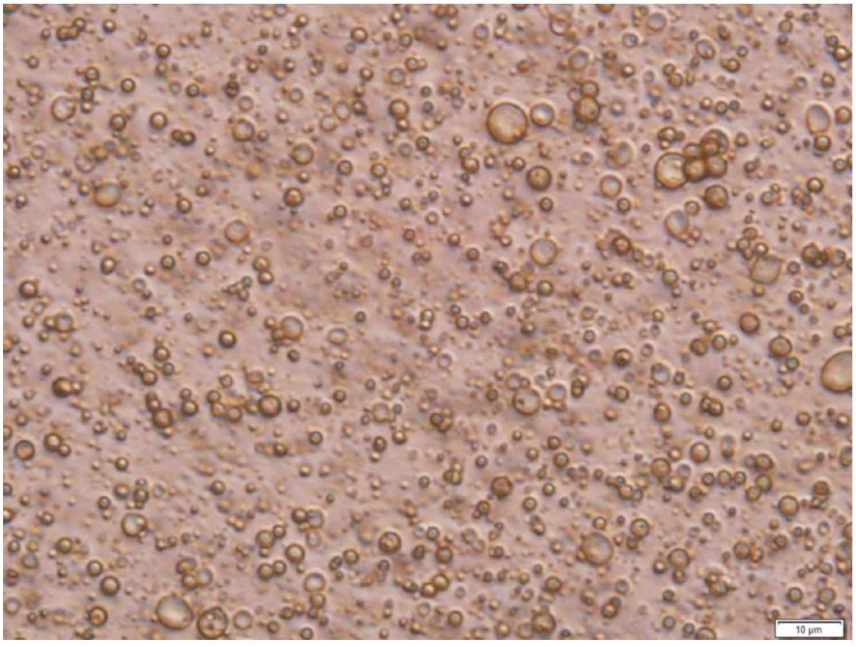

Figure 5.21 Optical Microscopic Image of the W/O Emulsion (Water-Oil Ratio of 80:20)

As can be seen, the three water-oil ratios generated the same type of emulsion, the water-in-oil (W/O) emulsion.

5.6.3 Emulsion Viscosity

The viscosities of the W/O emulsions for different water-oil ratios are listed in *Table 5.20*.

Table 5.20 W/O Emulsion Viscosities

Water-oil ratio	20:80	50:50	80:20
Viscosity, cP	204	>250 (equipment reading is 609)	N/A

As shown in the table, the viscosity of emulsions is measured and is higher than that of provided viscous oil.

The stability test for the generated emulsion indicates that the provided viscous oil may contain asphaltenes content, which is one of the naturally occurring stabilizing agents and one of the primary causes for production of stable W/O emulsion, as described in the previous work (Kokal and Al-Juraid 1998; Kokal 2002; Sun et al. 2016). Adsorption of asphaltenes onto water-oil interface may occur during emulsification that improves emulsion stability, which has been revealed by Filho et al. (2012). Additionally, confirmed by Kokal (2002) and Kilpatrick (2012), polar components remaining in provided viscous oil may lower the IFT of oil/water interface by forming anion of acid, which aids in the stabilization of W/O emulsion.

By comparing viscosities of W/O emulsion (with water-oil ratio of 20:80 and 50:50) and provided viscous oil, it is clear that the viscosity increases substantially with water cut as described earlier by Fu et al. (2012). Since the number of emulsion droplets per unit volume increases for water-oil ratio from 20:80 to 50:50, the viscosity increases. At higher water cut (80% water content), the viscosity of W/O emulsion cannot be measured. This could be due to sample and measurement differences as well as water droplet size distribution and transient nature of emulsions. The equation for calculating emulsion viscosity suggested by Kokal and Alvarez (2003) is also applied to calculate the viscosity of the generated W/O emulsion. And the calculated viscosity is close to the measured value when water-oil ratio is 50:50, which is 561.5 cp. The calculated viscosity of emulsion with water-oil ratio of 20:80 is lower than the measured value of 117.1 cp. This may be because the measured values are not accurate due to human errors such as parameters (e.g., temperature during the measurement and density of emulsion) that need to be set up precisely before each measurement as well as machine errors since the equipment was not calibrated before measurements.

Therefore, the lower value of endpoint of k_{rw} observed in the experimental trials may be a result of crude oil emulsification, which generates W/O emulsion with much higher viscosity. Thus, oil recovery may be improved by formation of W/O emulsion when LSW is injected into the reservoir, and may cause oil redistribution as well as mobilize the trapped oil and increase sweep efficiency, as corroborated by recent work (Emadi and Sohrabi 2013; Chakravarty et al. 2015; Arshad 2017).

5.7 Contact angle measurement

Figures 5.22 and *5.23* show the contact angle measurements. *Figure 5.22* illustrates the image of the contact angle between provided oil and reservoir rock in the presence of high salinity water, and the contact angle was read to be 105°. *Figure 5.23* illustrates the image of the contact angle between provided oil and reservoir rock in the presence of LSW, and the contact angle was read to be 130°.

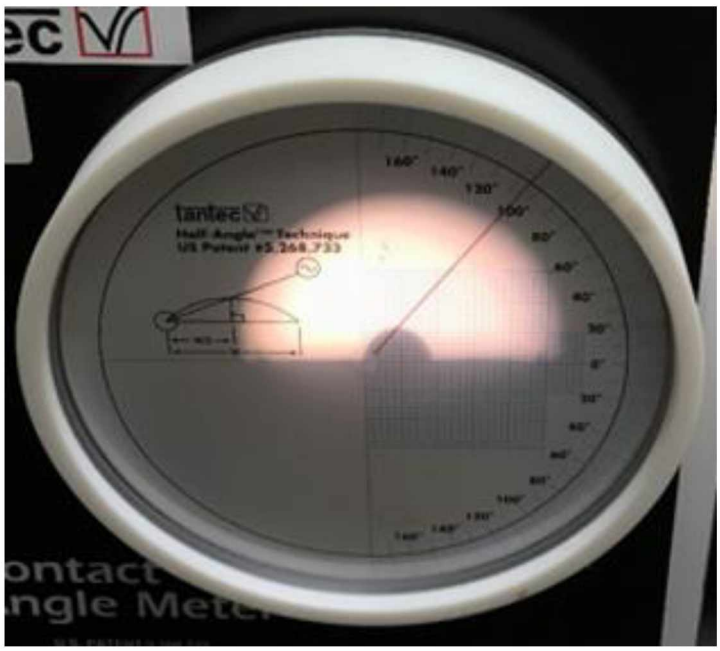

Figure 5.22 Contact Angle Between the Crude Oil and Reservoir Rock in the Presence of High Salinity Water

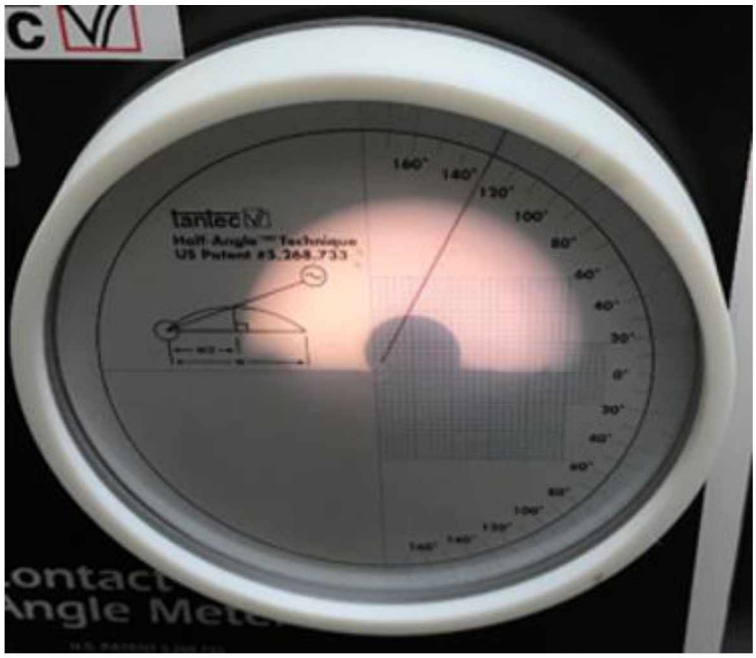

Figure 5.23 Contact Angle Between the Crude Oil and Reservoir Rock in the Presence of LSW

Based on Anderson's standard (1986), the wettability is classified as water-wet (0^o-75^o), mix-wet (75^o-115^o), and oil-wet (115^o-180^o), respectively. The contact angle change indicates that the wettability of rock surface may be changed toward more water-wet by contact with LSW. Injection of LSW induces wettability of rock surface from mixed-wet to water-wet. Then oil film becomes unstable and oil is released from rock surface. Thus, oil recovery is improved. Previous research conducted by Mugele (2016) implies that wettability alteration is one of the primary triggers for residual oil mobilization during LSWF. As described by Nasralla et al. (2016), LSW can alter the rock wettability toward more water-wet results in improved oil recovery. Similar results from Sanderson and Sohrabi (2014) provide a consistent explanation for wettability alteration (the wettability changes to be a more water-wet state) and the subsequent improved oil recovery based on fluid/fluid and rock/fluid interactions during LSW injection. In addition,

Teklu et al.'s research (2015) proved that wettability of rock surface increases with decreasing salinity, which may cause enhanced oil recovery. Furthermore, higher pH of LSW may also contribute to wettability change of rock surface during LSWF, which is proven by Buckley et al. (1996), who found that more water-wet condition should occur when rock surface is brought into contact with higher aqueous solution. Recently, investigations carried out by Sohrabi et al. (2017) and El-Yamani et al. (2017) revealed that polar components such as asphaltenes and resins remaining in the crude oil are responsible for wettability alteration during injection of LSW. The polar components are the cause for changing the initial wetness condition of rock surface to mixed-wet or oil-wet. The polar components are relocated and rearranged by contacting with LSW, which brings about formation of micro dispersion and reduces adhesion force between polar components and rock surface, resulting in desorption of crude oil from the rock surface. Thus, wettability of rock surface shifts toward a more water-wet state. A study (Kumar et al. 2005) used by atomic force microscopy (AFM) substantiates that wettability is controlled by the adsorption of polar components, which is very similar to that of crude oil.

6. Conclusions and Recommendations

6.1 Conclusions

Based on the aforementioned experimental results, the main findings of this study can be summarized as follows:

- The core plugs are very unconsolidated.
- After softening, the TDS of softened LSW showed little change, but the concentration of Ca^{2+} was reduced significantly. The Mg^{2+} concentration saw little change.
- The residual oil saturations are reduced successively by applying LSW flooding and softened LSW flooding after the high salinity water flooding.
- On average, after high salinity water flooding, LSW flooding can improve viscous oil recovery by 6.32%, while the softened LSW flooding can further enhance oil recovery by 1.26%.
- The pressure drops in the LSW flooding and softened LSW flooding are associated with more fluctuations than that in the high salinity water flooding, which indicates potential clay migration in the LSW flooding and softened LSW flooding.
- The calculated water relative permeabilities, especially the values of endpoint of k_{rw}, using the JBN method, are much lower than the typical values in the conventional systems, implying more complex reactions between the reservoir rock, viscous oil, and LSW. Also, it is found that water injection rate affects the k_{rw} values at the residual oil saturation.
- Stable emulsions were formed by mixing provided viscous oil and LSW.
- W/O emulsion can be formed by mixing provided viscous oil with LSW.

- The viscosity of the emulsion with a water-oil ratio of 20:80 was measured to be 204 cP, and the viscosity of the emulsion with a water-oil ratio of 50:50 was 609 cP, which are higher than that of the provided crude oil.
- The measured contact angle between the crude oil and reservoir rock in the presence of LSW is larger than that in the presence of high salinity water, indicating the rock surface wettability may be changed by contact with LSW.

6.2 Recommendations

It is recommended that, in the future, the following tasks be investigated:

1. The measured oil-water relative permeability curves are abnormal. The underlying reasons for the irregular oil-water relative permeability curves need to be further studied.
2. The LSWF has shown an average of 6% additional oil recovery, though its performance may be further improved by adding polymer, which needs further investigation.

References

Akin, S., & Demiral, M. R. B. (1997, January 1). Effect of Flow Rate on Imbibition Three-Phase Relative Permeabilities and Capillary Pressures. Society of Petroleum Engineers. doi:10.2118/38897-MS.

Al-Harrasi, A., Al-maamari Rashid Salim, & Masalmeh, S. K. (2012, January 1). Laboratory Investigation of Low Salinity Waterflooding for Carbonate Reservoirs. Society of Petroleum Engineers. doi:10.2118/161468-MS.

Al-Shalabi, E. W., Sepehrnoori, K., Delshad, M., & Pope, G. (2015, October 1). A Novel Method to Model Low-Salinity-Water Injection in Carbonate Oil Reservoirs. Society of Petroleum Engineers. doi:10.2118/169674-PA.

Alameri, W., Teklu, T. W., Graves, R. M., Kazemi, H., & AlSumaiti, A. M. (2014, October 14). Wettability Alteration During Low-Salinity Waterflooding in Carbonate Reservoir Cores. Society of Petroleum Engineers. doi:10.2118/171529-MS.

Alotaibi, M. B., & Nasr-El-Din, H. A. (2009, January 1). Salinity of Injection Water and Its Impact on Oil Recovery. Society of Petroleum Engineers. doi:10.2118/121569-MS.

Alotaibi, M. B., Azmy, R. M., & Nasr-El-Din, H. A. (2010, January 1). Wettability Studies Using Low-Salinity Water in Sandstone Reservoirs. Offshore Technology Conference. doi:10.4043/20718-MS.

Alshakhs, M. J., & Kovscek, A. R. (2015, September 28). An Experimental Study of the Impact of Injection Water Composition on Oil Recovery from Carbonate Rocks. Society of Petroleum Engineers. doi:10.2118/175147-MS.

Alshaikh, M., & Mahadevan, J. (2016, August 1). Impact of Brine Composition on Calcite Wettability: A Sensitivity Study. Society of Petroleum Engineers. doi:10.2118/172187-PA.

Anderson, W. G. (1986, October 1). Wettability Literature Survey- Part 1: Rock/Oil/Brine Interactions and the Effects of Core Handling on Wettability. Society of Petroleum Engineers. doi:10.2118/13932-PA.

Arshad, M. W., Loldrup Fosbøl, P., Shapiro, A., & Thomsen, K. (2017, October 15). Water-Oil Emulsions with Fines in Smart Water Enhanced Oil Recovery. Society of Petroleum Engineers. doi:10.2118/187620-MS.

Ashraf, A., Hadia, N., Torsaeter, O., & Tweheyo, M. T. (2010, January 1). Laboratory Investigation of Low Salinity Waterflooding as Secondary Recovery Process: Effect of Wettability. Society of Petroleum Engineers. doi:10.2118/129012-MS.

Attanasi, E.D. & Freeman, P.A. (2014, June 26) Evaluation of Development Options for Alaska North Slope Viscous and Heavy Oil Evaluation of Development Options for Alaska North Slope Viscous and Heavy Oil. Natural Resources Research.

Austad, T., Rezaeidoust, A., & Puntervold, T. (2010, January 1). Chemical Mechanism of Low Salinity Water Flooding in Sandstone Reservoirs. Society of Petroleum Engineers. doi:10.2118/129767-MS.

Austad, T., Sgariatpanahi, S.F., Strand S., Black, C.J.J., and Webb, K.J., 2012. Conditions for a low-salinity enhanced oil recovery (EOR) effect in carbonate oil reservoirs. Energy & Fuels. 26, 569-575.

Awan, A. R., Teigland, R., & Kleppe, J. (2008, June 1). A Survey of North Sea Enhanced-Oil-Recovery Projects Initiated During the Years 1975 to 2005. Society of Petroleum Engineers. doi:10.2118/99546-PA.

Batycky, J. P., McCaffery, F. G., Hodgins, P. K., & Fisher, D. B. (1981, June 1). Interpreting Relative Permeability and Wettability from Unsteady-State Displacement Measurements. Society of Petroleum Engineers. doi:10.2118/9403-PA.

Bedrikovetsky, P., Zeinijahromi, A., Badalyan, A., Ahmetgareev, V., & Khisamov, R. (2015, October 26). Fines-Migration-Assisted Low-Salinity Waterflooding: Field Case Analysis. Society of Petroleum Engineers. doi:10.2118/176721-MS.

Benavides, A. (2017, February 2). Prudhoe Bay: A 'Once-In-A-Lifetime Discovery'. E&P Hart Energy.

Bidinger, C. R., & Dillon, J. F. (1995, January 1). Milne Point Schrader Bluff: Finding the Keys to Two Billion Barrels. Society of Petroleum Engineers. doi:10.2118/30289-MS.

Buckley, J. S., Bousseau, C., & Liu, Y. (1996, September 1). Wetting Alteration by Brine and Crude Oil: From Contact Angles to Cores. Society of Petroleum Engineers. doi:10.2118/30765-PA.

Buckley, J. S., Liu, Y., & Monsterleet, S. (1998, March 1). Mechanisms of Wetting Alteration by Crude Oils. Society of Petroleum Engineers. doi:10.2118/37230-PA.

Buikema, T. A., Robbana, E., Mair, C., Williams, D., Mercer, D. J., Webb, K. J., Reddick, C. E. (2012, January 1). Low Salinity Enhanced Oil Recovery - Laboratory to Day One Field Implementation - LoSal^{TM} EOR into the Clair Ridge Project. Society of Petroleum Engineers. doi:10.2118/161750-MS.

Chakravarty, K. H., Fosbøl, P. L., & Thomsen, K. (2015, April 22). Interactions of Fines with Oil and its Implication in Smart Water Flooding. Society of Petroleum Engineers. doi:10.2118/173855-MS.

Chandrashegaran, P. (2015, August 4). Low Salinity Water Injection for EOR. Society of Petroleum Engineers. doi:10.2118/178414-MS.

Chmielowski, J. (2013). BP Alaska Heavy Oil Production from the Ugnu Fluvial-Deltaic Reservoir, Search and Discovery Article #80289. Pacific Section AAPG, SEG, and SEPM Joint Technical Conference.

Christensen, J. R., Stenby, E. H., & Skauge, A. (2001, April 1). Review of WAG Field Experience. Society of Petroleum Engineers. doi:10.2118/71203-PA.

El-Yamani, M. M., Sultan, A. S., & Al-Ramadan, K. A. (2017, June 1). Effect of Carbonate Microfacies on Contact Angle: Study from Middle Jurassic Tuwaiq Mountain Formation. Society of Petroleum Engineers. doi:10.2118/188132-MS.

Emadi, A., & Sohrabi, M. (2013, September 30). Visual Investigation of Oil Recovery by Low Salinity Water Injection: Formation of Water Micro-Dispersions and Wettability Alteration. Society of Petroleum Engineers. doi:10.2118/166435-MS.

Filho, D. C. M., Ramalho, J. B.V.S., Lucas, G. M.S., & Lucas, E. F. (2012). Aging of Water-In-Crude Oil Emulsions: Effect on Rheological Parameters. Colloids and Surfaces. ISSN 0927-7757.

Filoco, P. R., & Sharma, M. M. (1998, January 1). Effect of Brine Salinity and Crude Oil Properties on Relative Permeabilities and Residual Saturations. Society of Petroleum Engineers. doi:10.2118/49320-MS.

Fjelde, I., Asen, S. M., Omekeh, A., & Polanska, A. (2013, June 10). Secondary and Tertiary Low Salinity Water Floods: Experiments and Modeling. Society of Petroleum Engineers. doi:10.2118/164920-MS.

Fjelde, I., Omekeh, A. V., & Sokama-Neuyam, Y. A. (2014, April 12). Low Salinity Water Flooding: Effect of Crude Oil Composition. Society of Petroleum Engineers. doi:10.2118/169090-MS.

Fu, X., Lane, R. H., & Mamora, D. D. (2012, January 1). Water-in-Oil emulsions: flow in porous media and EOR potential. Society of Petroleum Engineers. doi:10.2118/162633-MS.

Guler, B., Wang, P., Delshad, M., Pope, G. A., & Sepehrnoori, K. (2001, January 1). Three- and Four-Phase Flow Compositional Simulations of CO2/NGL EOR. Society of Petroleum Engineers. doi:10.2118/71485-MS.

Gupta, R., Smith, G. G., Hu, L., Willingham, T., Lo Cascio, M., Shyeh, J. J., & Harris, C. R. (2011, January 1). Enhanced Waterflood for Carbonate Reservoirs - Impact of Injection Water Composition. Society of Petroleum Engineers. doi:10.2118/142668-MS.

Haagh, M. E. J., Siretanu, I., Duits, M. H. G., and Mugele, F. (2017, March 23). Salinity-Dependent Contact Angle Alteration in Oil/Brine/Silicate System: the Critical Role of Divalent Cations. American Chemical Society.

Heaviside, J., Brown, C. E., & Gamble, I. J. A. (1987, January 1). Relative Permeability for Intermediate Wettability Reservoirs. Society of Petroleum Engineers. doi:10.2118/16968-MS.

Jadhunandan, P. P., & Morrow, N. R. (1995, February 1). Effect of Wettability on Waterflood Recovery for Crude-Oil/Brine/Rock Systems. Society of Petroleum Engineers. doi:10.2118/22597-PA.

Jerauld, G. R., Webb, K. J., Lin, C.-Y., & Seccombe, J. (2006, January 1). Modeling Low-Salinity Waterflooding. Society of Petroleum Engineers. doi:10.2118/102239-MS.

Khataniar, S., Kamath, V. A., Patil, S. L., Chandra, S., & Inaganti, M. S. (1999, January 1). CO2 and Miscible Gas Injection for Enhanced Recovery of Schrader Bluff Heavy Oil. Society of Petroleum Engineers. doi:10.2118/54085-MS.

Kilpatrick, P. K. (2012, May 30). Water-in-Crude Oil Emulsion Stabilization: Review and Unanswered Questions. Energy Fuels. doi: 10.1021/ef3003262.

Kokal, S. (2002, January 1). Crude Oil Emulsions: A State-Of-The-Art Review. Society of Petroleum Engineers. doi:10.2118/77497-MS

Kokal, S., & Al-Juraid, J. (1998, January 1). Reducing Emulsion Problems By Controlling Asphaltene Solubility and Precipitation. Society of Petroleum Engineers. doi:10.2118/48995-MS.

Kokal, S., & Alvarez, C. (2003, January 1). Reducing Pressure Drop in Offshore Pipelines by Controlling the Viscosities of Pressurized Emulsions. Society of Petroleum Engineers. doi:10.2118/81511-MS.

Kulathu, S., Dandekar, A. Y., Patil, S., & Khataniar, S. (2013, October 22). Low Salinity Cyclic Water Floods for Enhanced Oil Recovery on Alaska North Slope. Society of Petroleum Engineers. doi:10.2118/165812-MS.

Kumar, K., Dao, E. K., & Mohanty, K. K. (2005, January 1). Atomic Force Microscopy Study of Wettability Alteration. Society of Petroleum Engineers. doi:10.2118/93009-MS.

Lager, A., Webb, K.J., Black, C.J.J., Singleton, M. and Sorbie, K.S., 2006. Low salinity oil recovery - an experimental investigation. Paper SCA2006-36 presented at the International Symposium of the Society of Core Analysts.

Lager, A., Webb, K. J., Black, C. J. J., Singleton, M., & Sorbie, K. S. (2008, February 1). Low Salinity Oil Recovery - An Experimental Investigation1. Society of Petrophysicists and Well-Log Analysts.

Leach, R. O., Wagner, O. R., Wood, H. W., & Harpke, C. F. (1962, February 1). A Laboratory and Field Study of Wettability Adjustment in Water Flooding. Society of Petroleum Engineers. doi:10.2118/119-PA.

Li, D., Kumar, K., & Mohanty, K. K. (2003, January 1). Compositional Simulation of WAG Processes for a Viscous Oil. Society of Petroleum Engineers. doi:10.2118/84074-MS.

Ligthelm, D. J., Gronsveld, J., Hofman, J., Brussee, N., Marcelis, F., & van der Linde, H. (2009, January 1). Novel Waterflooding Strategy by Manipulation of Injection Brine Composition. Society of Petroleum Engineers. doi:10.2118/119835-MS.

McKean, T. A. M., Thomas, A. H., Chesher, J. R., & Weggeland, M. C. (1999, January 1). Schrader Bluff CO2 EOR Evaluation. Society of Petroleum Engineers. doi:10.2118/54619-MS.

McGuire, P. L., Chatham, J. R., Paskvan, F. K., Sommer, D. M., & Carini, F. H. (2005, January 1). Low Salinity Oil Recovery: An Exciting New EOR Opportunity for Alaska's North Slope. Society of Petroleum Engineers. doi:10.2118/93903-MS.

McGuire, P. L., Redman, R. S., Jhaveri, B. S., Yancey, K. E., & Ning, S. X. (2005, January 1). Viscosity Reduction WAG: An Effective EOR Process for North Slope Viscous Oils. Society of Petroleum Engineers. doi:10.2118/93914-MS.

Morrow, N. R. (1975, October 1). The Effects of Surface Roughness On Contact: Angle With Special Reference to Petroleum Recovery. Petroleum Society of Canada. doi:10.2118/75-04-04

Morrow, N., & Buckley, J. (2011, May 1). Improved Oil Recovery by Low-Salinity Waterflooding. Society of Petroleum Engineers. doi:10.2118/129421-JPT.

Morrow, N. R., Cram, P. J., & McCaffery, F. G. (1973, August 1). Displacement Studies in Dolomite With Wettability Control by Octanoic Acid. Society of Petroleum Engineers. doi:10.2118/3993-PA.

Mugele, F., Siretanu, I., Kumar, N., Bera, B., Wang, L., de Ruiter, R., Collins, I. (2016, August 1). Insights From Ion Adsorption and Contact-Angle Alteration at Mineral Surfaces for Low-Salinity Waterflooding. Society of Petroleum Engineers. doi:10.2118/169143-PA.

Muggeridge, A., Cockin, A., Webb, K., Frampton, H., Collins, I., Moulds, T., Salino, P. (2013, December 2). Recovery Rates, Enhanced Oil Recovery and Technological Limits. DOI: 10.1098/rsta.2012.0320.

Nasralla, R. A., Bataweel, M. A., & Nasr-El-Din, H. A. (2011, January 1). Investigation of Wettability Alteration by Low Salinity Water. Society of Petroleum Engineers. doi:10.2118/146322-MS.

Nasralla, R. A., Sergienko, E., Masalmeh, S. K., van der Linde, H. A., Brussee, N. J., Mahani, H., Alqarshubi, I. (2014, November 10). Demonstrating the Potential of Low-Salinity Waterflood to Improve Oil Recovery in Carbonate Reservoirs by Qualitative Coreflood. Society of Petroleum Engineers. doi:10.2118/172010-MS.

Nasralla, R. A., Sergienko, E., Masalmeh, S. K., van der Linde, H. A., Brussee, N. J., Mahani, H., Al-Qarshubi, I. S. M. (2016, October 1). Potential of Low-Salinity Waterflood To Improve Oil Recovery in Carbonates: Demonstrating the Effect by Qualitative Coreflood. Society of Petroleum Engineers. doi:10.2118/172010-PA.

Nassir, M., Walters, D., Yale, D. P., Chivvis, R., & Turak, J. (2015, June 9). Coupled Reservoir and Geomechanical Modeling of Sand Production in Waterflooding of Heavy Oil Reservoirs. Society of Petroleum Engineers. doi:10.2118/174425-MS.

Ning, S. X., Jhaveri, B. S., Jia, N., Chambers, B., & Gao, J. (2011, January 1). Viscosity Reduction EOR with CO2 & Enriched CO2 to Improve Recovery of Alaska North Slope Viscous Oils. Society of Petroleum Engineers. doi:10.2118/144358-MS.

Paskvan, F., Turak, J., Jerauld, G., Gould, T., Skinner, R., & Garg, A. (2016, May 23). Alaskan Viscous Oil: EOR Opportunity, or Waterflood Sand Control First? Society of Petroleum Engineers. doi:10.2118/180463-MS.

Pospisil, G. (2011, January 6). Heavy Oil vs Light Oil. Alaska Oil and Gas Association.

Pu, H., Xie, X., Yin, P., & Morrow, N. R. (2008, January 1). Application of Coalbed Methane Water to Oil Recovery from Tensleep Sandstone by Low Salinity Waterflooding. Society of Petroleum Engineers. doi:10.2118/113410-MS.

Pu, H., Xie, X., Yin, P., & Morrow, N. R. (2010, January 1). Low-Salinity Waterflooding and Mineral Dissolution. Society of Petroleum Engineers. doi:10.2118/134042-MS.

Rapoport, L. A., & Leas, W. J. (1953, May 1). Properties of Linear Waterfloods. Society of Petroleum Engineers. doi:10.2118/213-G.

Rezaeidoust, A., Puntervold, T., & Austad, T. (2010, January 1). A Discussion of the Low-Salinity EOR Potential for a North Sea Sandstone Field. Society of Petroleum Engineers. doi:10.2118/134459-MS.

Romanuka, J., Hofman, J., Ligthelm, D. J., Suijkerbuijk, B., Marcelis, F., Oedai, S., Austad, T. (2012, January 1). Low Salinity EOR in Carbonates. Society of Petroleum Engineers. doi:10.2118/153869-MS.

Sanderson, C., & Sohrabi, M. (2014, November 1). Visualizing Low-Salinity Waterflooding. Society of Petroleum Engineers. doi:10.2118/1114-0032-JPT.

Seccombe, J., Akkurt, R., & Smith, M. (2005, January 1). Oil viscosity ranking in heavy oil reservoirs. Society of Petrophysicists and Well-Log Analysts.

Seccombe, J., Lager, A., Jerauld, G., Jhaveri, B., Buikema, T., Bassler, S., Fueg, E. (2010, January 1). Demonstration of Low-Salinity EOR at Interwell Scale, Endicott Field, Alaska. Society of Petroleum Engineers. doi:10.2118/129692-MS.

Shehata, A. M., & Nasr El-Din, H. A. (2015, April 27). Spontaneous Imbibition Study: Effect of Connate Water Composition on Low-Salinity Waterflooding in Sandstone Reservoirs. Society of Petroleum Engineers. doi:10.2118/174063-MS.

Shehata, A. M., & Nasr-El-Din, H. A. (2017, February 1). Laboratory Investigations to Determine the Effect of Connate-Water Composition on Low-Salinity Waterflooding in Sandstone Reservoirs. Society of Petroleum Engineers. doi:10.2118/171690-PA.

Shehata, A. M., & Nasr-El-Din, H. A. (2017, February 1). The Role of Sandstone Mineralogy and Rock Quality in the Performance of Low-Salinity Waterflooding. Society of Petroleum Engineers. doi:10.2118/181754-PA.

Sheng, J. J., (2014). Ctritical Review of Low-Salinity Waterflooding. Journal of Petroleum Science and Engineering.

Skauge, A., Thorsen, T., & Sylte, A. (2001). Rate Selection for Waterflooding of Intermediate Wet Cores. SCA 2001-20.

Sohrabi, M., Mahzari, P., Farzaneh, S. A., Mills, J. R., Tsolis, P., & Ireland, S. (2017, April 1). Novel Insights into Mechanisms of Oil Recovery by Use of Low-Salinity-Water Injection. Society of Petroleum Engineers. doi:10.2118/172778-PA.

Soraya, B., Malick, C., Philippe, C., Bertin, H. J., & Hamon, G. (2009, January 1). Oil Recovery by Low-Salinity Brine Injection: Laboratory Results on Outcrop and Reservoir Cores. Society of Petroleum Engineers. doi:10.2118/124277-MS.

Sufi, A. H., Ramey, H. J., & Brigham, W. E. (1982, January 1). Temperature Effects on Relative Permeabilities of Oil-Water Systems. Society of Petroleum Engineers. doi:10.2118/11071-MS.

Sun, M., Mogensen, K., Bennetzen, M., & Firoozabadi, A. (2016, October 1). Demulsifier in Injected Water for Improved Recovery of Crudes That Form Water/Oil Emulsions. Society of Petroleum Engineers. doi:10.2118/180914-PA.

Tang, G. Q. and Morrow, N. R., 1999. Influence of brine composition and fines migration on crude oil/brine/rock interactions and oil recovery. Journal of Petroleum Science of Engineering. 24: 99-111.

Targac, G. W., Redman, R. S., Davis, E. R., Rennie, S. B., McKeever, S. O., & Chambers, B. C. (2005, January 1). Unlocking the Value in West Sak Heavy Oil. Society of Petroleum Engineers. doi:10.2118/97856-MS.

Teklu, T. W., Alameri, W., Kazemi, H., & Graves, R. M. (2015, July 20). Contact Angle Measurements on Conventional and Unconventional Reservoir Cores. Unconventional Resources Technology Conference. doi:10.15530/URTEC-2015-2153996.

Torabzadey, S. J. (1984, January 1). The Effect of Temperature and Interfacial Tension on Water/Oil Relative Permeabilities of Consolidated Sands. Society of Petroleum Engineers. doi:10.2118/12689-MS.

United States. Dept. of the Interior. (1973). Final Environmental Statement for the Geothermal Leasing Program: Leasing of Geothermal Resources in Three California Areas.

Wagner, O. R., & Leach, R. O. (1959, December 1). Improving Oil Displacement Efficiency by Wettability Adjustment. Society of Petroleum Engineers. doi:10.2118/1101-G.

Webb, K. J., Lager, A., and Black C. J. J., (2007). Impact of brine chemistry on oil recovery. Paper A24 presented at the 14th European Symposium on Improved Oil Recovery, Cairo, Egypt, 22-24 April.

Xu, W. (2005). Experimental Investigation of Dynamic Interfacial Interactions at Reservoir conditions, MSc. Thesis, Louisiana, USA.

Yang, J., Dong, Z., and Lin, M., 2015. The impact of brine composition and salinity on the wettability of sandstone. Petroleum Science and Technology.

Yi, Z., & Sarma, H. K. (2012, January 1). Improving Waterflood Recovery Efficiency in Carbonate Reservoirs through Salinity Variations and Ionic Exchanges: A Promising Low-Cost "Smart-Waterflood" Approach. Society of Petroleum Engineers. doi:10.2118/161631-MS.

Yidliz, H., Morrow, N. R., and Valat, M. (1996, January 1). Effect of Brine Composition On Recovery of an Alaskan Crude Oil by Waterflooding. Petroleum Society of Canada. doi:10.2118/96-94.

Young, J. P., Mathews, W. L., & Hulm, E. (2010, January 1). Alaskan Heavy Oil: First CHOPS at a vast, untapped arctic resource. Society of Petroleum Engineers. doi:10.2118/133592-MS.

Yousef, A. A., Al-Saleh, S. H., Al-Kaabi, A., & Al-Jawfi, M. S. (2011, October 1). Laboratory Investigation of the Impact of Injection-Water Salinity and Ionic Content on Oil Recovery from Carbonate Reservoirs. Society of Petroleum Engineers. doi:10.2118/137634-PA.

Yousef, A. A., Al-Saleh, S., & Al-Jawfi, M. S. (2012, January 1). Improved/Enhanced Oil Recovery from Carbonate Reservoirs by Tuning Injection Water Salinity and Ionic Content. Society of Petroleum Engineers. doi:10.2118/154076-MS.

Zahid, A., Shapiro, A. A., & Skauge, A. (2012, January 1). Experimental Studies of Low Salinity Water Flooding Carbonate: A New Promising Approach. Society of Petroleum Engineers. doi:10.2118/155625-MS.

Zeinijahromi, A., Ahmetgareev, V., & Bedrikovetsky, P. (2015, October 20). Case Study of 25 Years of Low Salinity Water Injection. Society of Petroleum Engineers. doi:10.2118/176128-MS.

Zekri, A. Y., Nasr, M., Al-Arabai, Z., 2012. Effect of EOR Technology on Wettability and Oil Recovery of Carbonate and Sandstone Formation. IPTC 14131 presented at the International Petroleum Technology Conference, Bangkok, Thailand, 7–9 February.

Zhang, Y., Xie, X., & Morrow, N. R. (2007, January 1). Waterflood Performance by Injection of Brine with Different Salinity for Reservoir Cores. Society of Petroleum Engineers. doi:10.2118/109849-MS.